Appendix A

EQUATIONS NECESSARY FOR DESCRIPTION OF LNAPL SOURCE AND TRANSPORT

A.1 DEFINITIONS OF HEAD AND PRESSURE RELATED TO CAPILLARY BATH AND SOIL PORE ANALOGY:

$$H = Z + \frac{P}{\rho g} \quad (1) \qquad P_c = P_n - P_w \quad (2) \qquad h_c = \frac{P_c}{\rho g} \quad (3) \qquad P_c = \frac{2\sigma}{r_c} \quad (4)$$

Where H = total head, Z = elevation, P = pressure, P_c = capillary pressure, P_n = pressure in nonwetting phase, P_w = pressure in wetting phase, σ = the interfacial tension between the fluid pairs, r_c is the radius of curvature of the pore throat, h_c = capillary pressure head, ρ = fluid density 1.0 g/cc when referenced to the water phase as all couplets are for convenience and consistency.

And noting that the capillary rise between each capillary couplet is dependent on the interfacial tension (IFT), we can develop the following scaling relationships between couplets referenced to the water system by equation 4 above.

$$P_c^{aw} = \frac{2\sigma_{ow}}{r} \quad (5) \qquad P_c^{ow} = \frac{2\sigma_{ow}}{r} \quad (6) \qquad P_c^{ao} = \frac{2\sigma_{ao}}{r} \quad (7)$$

Since the pore radius of curvature is equal for each of these relationships, we can rewrite to scale the capillary rise of one system (we will assume air/water) to any of the other systems. Recall the definition of capillary head above (Equation 3), with each couplet referenced to the air/water system.

$$h_c^{ij} = \frac{2\sigma_{ij}}{\rho_w g r} \quad (8) \qquad h_c^{ao} = h_c^{aw}\frac{\sigma_{ao}}{\sigma_{aw}} \quad (9) \qquad h_c^{ow} = h_c^{aw}\frac{\sigma_{ow}}{\sigma_{aw}} \quad (10)$$

This scaling relationship can be used to take the air/water capillary data measured in a lab and scale it to the oil/water or air/oil fluid systems. The new curves are then refit by a capillary function to define the capillary parameters for that new couplet (e.g., equations 12 & 13 below, van Genuchten [VG] and Brooks Corey [BC] functions). Alternatively, a simpler approach is to note that the pore radius is the key factor for this conversion and, therefore, one should be able to scale the capillary rise or bubbling pressure parameter accordingly (Farr et al., 1990); these are the parameters "α" for the VG equation, and "Ψ_b" for the BC equation that are discussed below.

A.2 DEFINITIONS OF SATURATION, VOLUMETRIC FLUID CONTENT, AND HEAD IN SOIL:

$$S_e = \frac{\theta - \theta_r}{\theta_m - \theta_r} \quad (11) \qquad S_e = \left[1+\left(\alpha_{ij} H_{c_{ij}}\right)^N\right]^{-m} \quad (12) \qquad S_e = \left[\frac{\Psi_{bij}}{\Psi_{c_{ij}}}\right]^{\lambda} \text{ for } \Psi_c > \Psi_b, \text{ else } S_e = 1.0 \quad (13)$$

$$h_{ow} = (1-\rho_{ro})\, Z_{ow} \quad (14) \qquad h_{ao} = (\rho_{ro})\, Z_{ao} \quad (15)$$

*Where $\mathbf{S_e}$ is the effective water saturation below the oil/air table and the total liquid saturation above the oil/air table; **i** & **j** denote the couplet of interest; Ψ_b is the Brooks-Corey bubbling pressure; λ is the BC pore size index; θ is the volumetric fluid content, with **r** & **m** subscripts indicating residual and maximum endpoints; α is a capillary parameter inversely related to the soil capillary rise; **N** is a capillary parameter related to the uniformity of pore throat distribution; m = 1-1/N; ρ_{ro} is the relative oil density scaled against water (specific gravity); $\mathbf{h_{ow}}$ and $\mathbf{h_{ao}}$ are the oil/water and air/oil capillary heads.*

Between the oil/water and oil/air interfaces, we have a two-phase system of oil and water controlled by the oil-water capillary parameters. Above the oil/air interface, we have a 3-phase system controlled by the air/oil and oil/water water parameters. And above the oil capillary fringe, we revert back to an air-water capillary system.

$$Vo = \Theta_e \int_0^{surf} S_o\, dz \quad (16)$$

The oil saturation profile corresponding to some observed oil thickness, is calculated using the capillary relationships above. The total oil volume (V_o - Equation 16) per unit area is simply the vertical integral of the oil saturation profile multiplied by the effective porosity ($\Theta_e = \Theta_t - \Theta_r$). It is also possible to rewrite the VG and BC equations above to explicitly account for the residual water saturation, in which case the total porosity would be used for the volume/area integration. The calculations in the toolkit account for this factor in calculating the total LNAPL and component mass used for the transport calculations. Whether using the VEQ approximation, or some other oil distribution defined by the user or approximated by a recovery calculation (see Appendix B), the evaluation method integrates the volume per area over the area of the plume as defined by the user input.

A.3 DEFINITIONS OF CONDUCTIVITY, RELATIVE PERMEABILITY, EFFECTIVE CONDUCTIVITY AND TRANSMISSIVITY

$$K = k_i \frac{\rho g}{\mu} \quad (17) \qquad K_{eff} = k_r\, k_i \frac{\rho g}{\mu} \quad (18) \qquad T_{eff} = \frac{k_i\, \rho_o\, g}{\mu_o} \int_0^{Z_o} k_{ro}\, z \quad (19)$$

$$k_{ro} = \left(S_o\right)^{0.5} \left[\left(1 - S_w^{1/m}\right)^m - \left(1 - S_t^{1/m}\right)^m\right]^2 \quad (20) \qquad k_{rw} = S_w^{1/2} \left[1 - \left(1 - S_w^{1/m}\right)^m\right]^2 \quad (21)$$

$$k_{ra} = \left(1 - S_t\right)^{1/2} \left(1 - S_t^{1/m}\right)^{2m} \quad (22)$$

*Where kr = is relative permeability with respect to w - water, o -oil (LNAPL), a -air phases (Mualem, 1976; Parker, 1989), S = phase saturation (t - total, w - water, o - oil), m = 1-1/N where **N** is a capillary parameter, as defined above.*

$$q_p = -K_{eff_p} i_p \quad (23) \qquad q_{pi} = -\frac{k_{rp} k_{ij}}{\mu_p}\left[\frac{\partial P_p}{\partial x_j} + \rho_p g \frac{\partial z}{\partial x_j}\right] \quad (24)$$

*Darcy's Law may be written in 2 forms: where **i** and **j** are direction indices with repeated values indicating tensor notation, **p** is an index indicating fluid phase, $\mathbf{q_{pi}}$ is the Darcy velocity, $\mathbf{k_{rp}}$ is the relative permeability scalar, $\mathbf{k_{ij}}$ is the intrinsic permeability tensor of the soil, μ_p is viscosity, P_p is the pressure, ρ_p is the density, **g** is gravitational acceleration, **z** is elevation.*

The mass conservation equation is necessary to account for changes in fluid movement in any phase and any direction [eq. A-2]. The equation mathematically states that a change in flux in any given direction must be equaled by a change in fluid storage in the corresponding elemental pore space.

$$\frac{\delta q_{pi}}{\delta x_j} = \frac{\delta}{\delta t}\left(\theta_e \rho_p S_p\right) - M_p \quad (25)$$

*Where **t** is time, θ_p is effective porosity, ρ is density, **S** is phase saturation, and $\mathbf{M_p}$ is a source/sink term with respect to phase **p** accounting for pumping, injection, or other boundary functions, and **x** indicates the Cartesian direction of the differential equation.*

Groundwater Flux

The volumetric groundwater flux (q) below and within the LNAPL pool varies as a function of the background or regional specific discharge (q_{max}) and the water saturation. Below the LNAPL/water interface, the groundwater flux is equal to the regional specific discharge. Above the groundwater piezometric surface, or corrected water table (defined as elevation where the groundwater pressure is equal to zero), there is no horizontal groundwater flux. Between the LNAPL/water interface and the groundwater piezometric surface, the groundwater specific discharge is given by:

$$q = k_{rw} k_i \frac{\rho_w g}{\mu} i \quad (26)$$

*where $\mathbf{k_{rw}}$ is the relative permeability of the wetting phase (water), $\mathbf{k_i}$ is the intrinsic permeability of the soil, ρ_w is the density of water, μ is the viscosity of water, and **i** is the hydraulic gradient.*

Recognizing that the background or regional specific discharge (q_{max}) is given by:

$$q_{max} = k_i \frac{\rho_w g}{\mu} i \quad (27)$$

equation (26) can be rewritten as $q = k_{rw}\, q_{max}$, or $\frac{q}{q_{max}} = k_{rw}$, where the relative permeability, k_{rw} was given above. In a multilayer case, q_{max} through each zone is defined by the permeability or conductivity of that horizon. The water fluxes from each layer are summed to give the total flux across the zone. The above equations can be used to calculate the ratio of groundwater flux through the LNAPL zone (q) to the regional flow q_{max}.

Constituent Concentrations

Above the LNAPL/water interface, groundwater flowing through the soil is in direct contact with LNAPL, so the equilibrium concentration of a soluble constituent in a multicomponent LNAPL is simply given by an analogy to Raoult's Law:

$$C_{eff\,m} = x_m\, C_{sol\,m} \quad (28)$$

where $\mathbf{C_{eff_m}}$ *is the effective solubility of the* **m**, *compound,* $\mathbf{x_m}$ *is the mole fraction and* $\mathbf{C_{sol_m}}$ *is the pure phase solubility of compound* **m**.

The mole fraction x_m is also applied, at the user's option, to calculate the vapor phase concentration and loss from the system for volatile components. Similar to the water phase, Raoult's Law for the gas phase may be written:

$$C_{veff} = \frac{x_m\, VP_m\, MW_m}{R\,T} \quad (29)$$

where $\mathbf{C_{veff}}$ *is the effective vapor concentration (mg/l),* $\mathbf{VP_m}$ *is the pure phase vapor pressure,* $\mathbf{MW_m}$ *is the molecular weight of the pure component,* **R** *is the ideal gas constant (0.0821 mol-l/atm) and* **T** *is temperature (**K**).*

Below the LNAPL/water interface, the concentration is controlled by vertical downward diffusion of the soluble constituent. This process is discussed extensively by Johnson and Pankow (1992), which, in turn, is based on the work of Hunt et al., (1988). These authors show that the concentration (C) above a DNAPL pool (or analogously below an LNAPL pool) is given by:

$$\frac{C}{C_{eff}} = erfc\left[\frac{z}{2\left(\frac{D_v L_p}{\bar{v}}\right)^{1/2}}\right] \quad (30)$$

where $\mathbf{z}$ *is the distance below the LNAPL/water interface,* $\mathbf{L_p}$ *is the length of the pool along the groundwater flow direction,* $\bar{v}$ *is the groundwater flow velocity (=* q/ϕ*), and* $\mathbf{D_v}$ *is the vertical dispersion coefficient, given by* $D_v = D_e + \bar{v}\alpha_v$*, where* $\mathbf{D_e}$ *is the effective aqueous molecular diffusion coefficient, and* α_v *is the vertical dispersivity.* For a layered condition, this same chemical dispersion is allowed between adjacent soil zones.

Mass Flux

There are three potential components to mass flux, as suggested from the equations above: 1) Solubilization and transport within the LNAPL zone later rejoining the regional flow field; 2) Diffusion below the LNAPL lens and transport at the regional flow rate; 3) Volatilization of components through the vadose zone.

Beginning with the soluble phases, the above calculations of aqueous concentration distribution can be combined with the calculated groundwater flux, resulting in the mass flux distribution, by noting that the mass flux (j) is given by (31):

$$j = q\,C \quad (31)$$

This soluble mass flux can be normalized to the maximum mass flux, which is simply the product of the regional specific discharge (q_{max}) multiplied by the effective solubility of the constituent of concern (C_{eff}). The total mass flux depleting the LNAPL source is simply the vertical integral of eq. (31) across the LNAPL zone multiplied by a unit width of the pool, including zones of layering where q varies because of soil properties. Above the LNAPL/water interface, the concentration of the soluble phase is constant with height, so the total mass flux (J_1) per unit width of LNAPL pool is given as:

$$J_1 = C_{eff} \int_0^{z_{wt}} q(z)\,dz \quad (32)$$

where $\mathbf{z_{wt}}$ *is the elevation of the groundwater piezometric surface (or corrected water table).*

Because the water saturation profile, and therefore the relative permeability profile and flux, cannot be integrated analytically, equation (32) must be numerically evaluated by piecewise summation. Below the LNAPL/water interface, as noted above, the groundwater flux (q) remains constant while the concentration varies. Thus, the total mass flux below the interface (J_2) is given as:

$$J_2 = q \int_{-\infty}^{0} C(z)\, dz \quad (33)$$

The distribution of concentration as a function of depth below the LNAPL/water interface is given by equation (30) and can be integrated analytically, resulting in;

$$J_2 = C_{eff} \sqrt{4 D_v\, q\, \phi\, L_p / \pi} \quad (34)$$

The total mass flux in the water phase from both factors is simply $J_1 + J_2$. This distributed flux is used to track losses from the LNAPL phase. The zones through and below the LNAPL are discretized into 100-layer wise pieces. For as long as there is flux and chemical mass within a layer, the corresponding effective concentration of a compound of concern in that zone is used as input to the Domenico 2-dimensional groundwater transport equation (Domenico & Schwartz, 1990). As mass is depleted in a zone, only the diffusive portion of concentration is used as input.

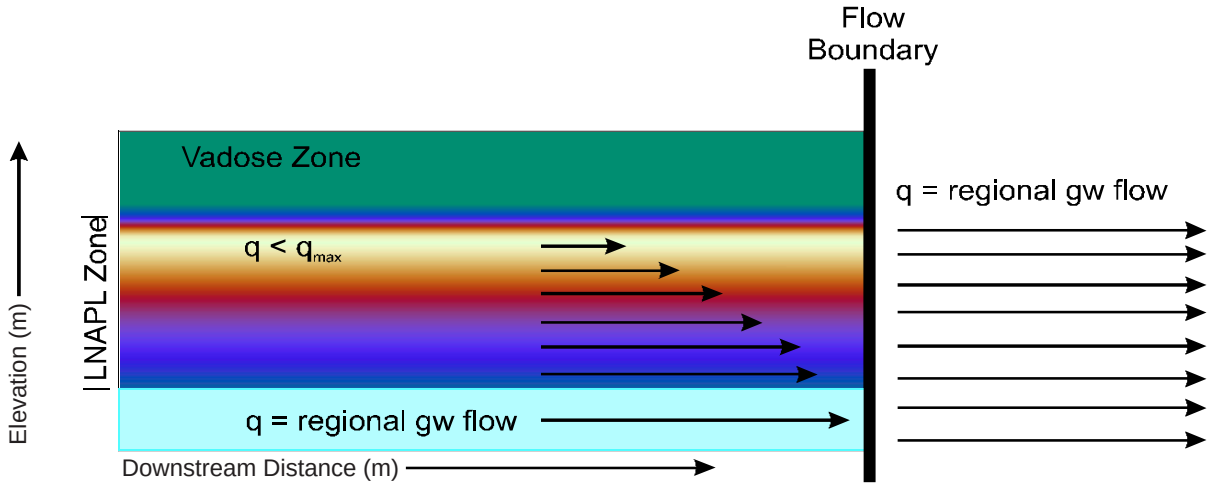

Figure A-1. Cross-section view of groundwater flow through & below the LNAPL interval and the boundary that results for the transport condition.

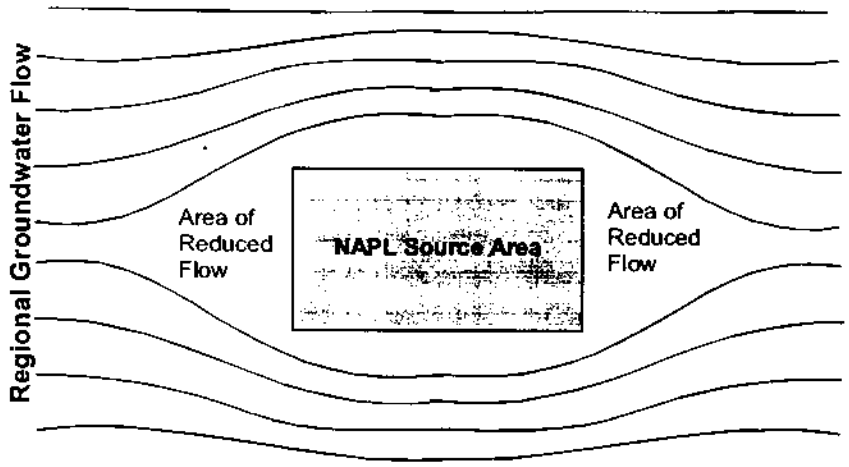

Figure A-2. Plan view of groundwater flow lines that will diverge and then converge around an LNAPL source area, that is in effect, a zone of overall lower hydraulic conductivity toward water.

Invoking analytic assumptions results in a numerical discontinuity at the front of the LNAPL source zone. At this boundary, the regional groundwater flux changes from a slowed condition in the LNAPL interval to regional conditions assumed for the transport algorithm (see figures A-1 and A-2). As concentration is the input to the transport solution, this means that there is a flux discontinuity at this boundary that results in somewhat greater predicted concentrations that may be evident under field conditions. The flux is tracked through the LNAPL zone, so the discontinuity becomes less important through time as mass is depleted from the system. Since the discontinuity results in an overestimate of concentrations in groundwater immediately ahead of the source zone, the analytic boundary condition is conservative (i.e., worst-case).

Turning to the vapor phase, the flux is assumed to occur under ambient (non-flowing) conditions and is therefore diffusion gradient driven. This flux modifies the remaining mass in the LNAPL source of any particular component through time, in turn modifying the source concentration term for groundwater. It is assumed that the ground surface is a zero concentration boundary, and at steady-state, one may calculate the concentration flux using Fick's Law:

$$J_3 = E_v D_e \frac{dC}{dZ} \quad (35) \qquad\qquad D_e = D_a \frac{\theta_a^{3.33}}{\theta_t^2} \quad (36)$$

where $\boldsymbol{J_3}$ is the flux loss from volatilization, $\boldsymbol{E_v}$ is a volatilization efficiency (see below); $\boldsymbol{D_e}$ is the effective air diffusion coefficient (36), $\boldsymbol{Z}$ is depth, $\boldsymbol{D_a}$ is the free-air diffusion coefficient, θ_a is the air-filled porosity, and θ_t is the total porosity (Millington-Quirk, 1959).

The change in vapor concentration is simply the range between the Raoult's derived concentration above the source LNAPL at any particular time in the volatilization and zero at ground surface. Notice that because of capillarity, the θ_a is not constant, but varies with vertical position in accordance with the change in liquid content. For the calculations here, the effective diffusion coefficient

is calculated across the interval of diffusion as a weighted series (37):

$$D_e^* = \frac{Z_t}{\sum_{i=1}^{n=100} Z_i / D_e} \quad (37)$$

The user also has the option of providing a volatilization efficiency factor (E_v) that varies from 0 to 1.0, with zero being no diffusive losses and 1.0 being maximum losses. The factor is included so that real world conditions limiting vapor flux can be considered, as appropriate. Such conditions may include asphalt and concrete covers, zones of high relative wetness, and/or zones of geologic contrast.

The total mass loss of any compound from the LNAPL zone is simply the time integral of the sum of the fluxes subtracted from the initial mass in the LNAPL zone at the start of the calculation:

$$Mass_t = Mass_{init} - \left[\int_0^t J_1 dt + \int_0^t J_2 dt + \int_0^t J_3 dt \right] \quad (38)$$

where ***Mass***$_t$ *is the mass of any compound in the LNAPL at any time* ***t****.*

As the component specific mass is depleted, its mole fraction in the remaining product is reduced, as is its effective solubility and volatility by equations (28 & 29). This ever diminishing flux controls the longevity and strength of the LNAPL source and by implication, the risk. In the calculation utility provided in the toolkit, the change in mass through time (source depletion) is calculated and updated at each timestep to define the concentration input into the Domenico transport equation.

Appendix B

DERIVATION OF LNAPL RECOVERY EQUATIONS

Charbeneau et al., 1999
API Publication 4682

This appendix presents the derivation of recovery equations for oil recovery under a variety of conditions. The equations are modified after Charbeneau (1999), which the reader is encouraged to review for clarification of principles and assumptions. The key assumptions needed to develop these equations are as follows:

1) VEQ conditions are approximated at all times;
2) The spatial variability of recovery is not significant within the phase radius of influence;
3) Pumping recovery can be approximated by steady-state conditions;
4) Multiple recovery wells are simply additive;
5) The oil saturation profile diminishes through time, but is distributed uniformly throughout the ROI at any given time;
6) Volumetric recovery is proportional to change in saturation and LNAPL thickness;
7) The effective transmissivity toward LNAPL is dependent on the vertical integral of the relative permeability function, which depends on the saturation distribution at any time during recovery (see Appendix A);
8) The maximum endpoint to recovery is the field oil capacity (residual oil);
9) There is no recovery at equivalent oil thicknesses less than the bubbling pressure for the oil/water system.

Equation Development

We will use a simple radial recovery system as our basis for developing the recovery approximation method. The principles will then be extended to trench recovery as an alternate geometry, and to vacuum enhanced recovery as a gradient improvement without chemical stripping. Figure B-1 illustrates a skimming or dual-pump recovery well where both LNAPL and water are coned down from their initial thicknesses b_{oi} and b_{wi}. The air phase is assumed to be static and flow of LNAPL and water is steady. The thickness of the LNAPL and water layers is equal to b_{oi} and b_{wi}, respectively, at a distance R from the well. The distance R, therefore, is the well's hydraulic radius of influence. The wellbore has a radius of r_w.

Under these assumed conditions, the Thiem equation (1906) and Dupuit assumptions (1863) can be used to describe the recovery of fluids (water and oil) under steady radial pumping.

$$(H_i^2 - H_w^2) = \frac{Q}{\pi K} ln \frac{r_i}{r_w} \qquad\qquad Q = \frac{\pi K(H_i^2 - H_w^2)}{\ln \frac{r_i}{r_w}}$$

*Where **Q** is the volumetric flow rate, **K** is the conductivity, $\mathbf{r}_1$ is the radius of influence, $\mathbf{r}_w$ is the well radius, and **H** is the head. This form of the Thiem equation can be re-written in terms of flow.*

Focusing for now on oil flow, we know that for a multiphase system the average effective oil conductivity depends on the oil saturation profile and resultant relative permeability (Appendix A). As oil is incrementally recovered, that volume can be subtracted from the volume in place to result in a new average saturation and conductivity profile (Figure B-1, showing initial and changing saturation profiles during recovery, with Tr = relative transmissivity to show change in bulk mobility).

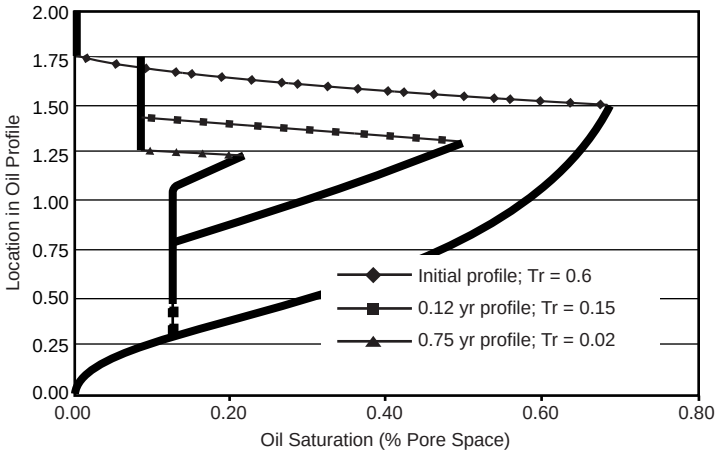

Figure B-1. Changes in LNAPL saturation profiles in response to continuing hydraulic recovery.

This principle can now be used to calculate the diminishing oil recovery through time. Each increment of recovery reduces the average conductivity, in turn diminishing the next increment of recovery. Note that the hydraulic conductivity toward water is scaled to the oil system by appropriate fluid properties.

I. Trench System

$$Q_o = W\, b_o\, \overline{k_{ro}}\, K_w\, \frac{r_{ro}}{\pi_{ro}}\, i$$

W = Width of trench (up to width of LNAPL source).
b_o = Thickness of LNAPL.
$\overline{k_{ro}}$ = Average relative permeability of LNAPL.
K_w = Water-saturated hydraulic conductivity of soil.

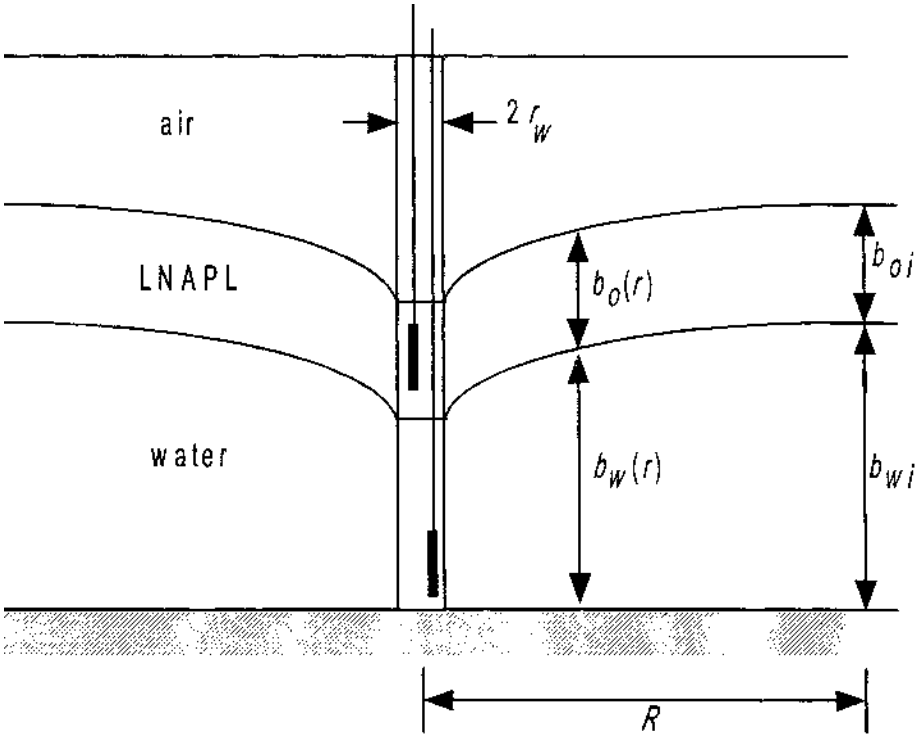

Figure B-2. Steady Incompressible Radial Flow of LNAPL and water to a Dual-Pumping Well in a Homogeneous Medium (after Charbeneau, 1999)

ρ_{ro} = Relative density of LNAPL.

μ_{ro} = Relative viscosity of LNAPL.

i = Gradient of LNAPL (assumed to be same as groundwater gradient).

The trench system assumes that lateral boundary effects can be ignored, and that flow is effectively 1-D for calculation purposes. All upgradient product will flow directly toward the recovery trench.

II. Skimmer well

$$Q_o = \frac{2\pi(1-\rho_{ro})\rho_{ro} b_o^2 K_w \overline{k_{ro}}}{\mu_{ro} \ln(r_i / r_w)}$$

r_i = Radius of influence of well.

r_w = Radius of well.

The skimmer well assumes that product drawdown is to the water piezometric surface. That is, all product from the well is removed to a "sheen", and the gradient is then this drawdown propagated across the radius of influence as defined by the Thiem equation.

III. Dual Pump/Total Fluids Recovery Well

$$Q_o = \frac{2\rho_{ro} b_o \overline{k_{ro}} Q_w}{\mu_{ro} b_w \left(1 + \sqrt{1 - \frac{Q_w}{\pi K_w b_w^2} ln \frac{r_i}{r_w}}\right)}$$

$$Q_w = \frac{(b_w^2 - h_{ow}^2)\pi K_w}{ln\left(R_w / r_w\right)}$$

Where $\mathbf{Q_o}$ *is oil production and* $\mathbf{Q_w}$ *is water.*

b_w = Distance from bottom of well screen to piezometric surface.
h_{ow} = Distance from bottom of well screen to oil-water interface.

IV. Vacuum Enhanced Skimmer Well

$$Q_o = \frac{2\pi(1-\rho_{ro})\rho_{ro} b_o^2 K_w \overline{k_{ro}}}{\mu_{ro} ln(r_i / r_w)} + \frac{\mu_a \rho_{ro} Q_a b_o \overline{k_{ro}}}{\mu_o k_{ra} L_a}$$

$$Q_a = \frac{s_a 2\pi L_a K_w k_{ra}}{\mu_{ra} ln\left(r_i / r_w\right)}$$

Where $\mathbf{Q_o}$ *is oil production, the first component equivalent to the skimmer well above, and the second component a gradient factor from the air flow component* $\boldsymbol{Q_a}$.

μ_{ra} = Relative viscosity of air.
L_a = Length of vacuum screen.
k_{ra} = Relative permeability of air phase.
s_a = Air drawdown (applied vacuum).

Lastly, for all the calculations above, an approximation derived by Charbeneau (1999) is used to simplify calculation of the relative permeability function.

$$\overline{k_{ro}} = \left(\overline{S_o}\right)^2 \qquad \left(\overline{S_o}\right) = \frac{V_o}{nb_o}$$

Where $\mathbf{S_o}$ is the average oil saturation calculated by the area volume ($\mathbf{V_o}$) divided by the porosity ($\mathbf{n}$) and oil thickness interval ($\mathbf{b_o}$)

IMPLEMENTATION

The equations above are implemented to act upon a user selected VEQ distribution of LNAPL. The time increments of calculation are selected such that no more than 25% of the oil in place is recovered during any single timestep. The recovered oil causes the saturation profile to move upward, leaving behind residual oil along the way (Figure B-1). Therefore, of the initial oil in place, some fraction (the area and vertical integral of the user selected residual oil) will be permanently unrecoverable. The time to reach asymptotic or residual state depends on the hydraulic conductivity of the soil, the gradient applied, and the average saturation of oil in place.

Given this and the simple form of the approximation, it is not surprising that all cleanup methods reach the same endpoint, residual saturation. The only difference between remediation techniques or the specifics of the setting is the time required to reach that endpoint. In practicality, complications of well field mechanics, interference, well operations, and hydraulic variability will result in slower cleanup times and greater variability in effectiveness than estimated by this method. These calculations are best-case and for screening purposes only.

Appendix C

SOIL, FLUID, AND CHEMICAL PROPERTIES FROM VARIOUS SOURCES

SOIL PROPERTIES

Source:

Charbeneau, Randall (1999). Free Product Recovery of Petroleum Hydrocarbon Liquids, prepared for American Petroleum Institute.

Table C-1. Typical Value of Hydraulic Conductivity (after Marsily, 1986).

Medium	***K* (cm/s)**
Unconsolidated Material	
Coarse gravel	10^{1} - 10^{0}
Sands and gravel	10^{0} - 10^{-3}
Fine sand, silt, and loess	10^{-3} - 10^{-7}
Clay, shale,and glacial till	10^{-7} - 10^{-11}
Unfractured Rock	
Dolomitic limestone	10^{-1} - 10^{-3}
Weathered chalk	10^{-1} - 10^{-3}
Unweathered chalk	10^{-4} - 10^{-7}
Limestone	10^{-3} - 10^{-7}
Sandstone	10^{-2} - 10^{-8}
Granite, gneiss, and basalt	10^{-7} - 10^{-11}

Table C-2. Hydraulic Conductivity of Different Soil Texture Classes from the Data Set of Carsel and Parish (1988).

mean (standard deviation)

	K_w	K_w
Soil Type	(cm/s)	(m/day)
Clay	5.56E-05	0.0048 (0.10)
Clay Loam	7.22E-05	0.062 (0.17)
Loam	2.89E-04	0.25 (0.44)
Loamy Sand	4.05E-03	3.5 (2.7)
Silt	6.94E-05	0.060 (0.079)
Silt Loam	1.25E-04	0.11 (0.30)
Silty Clay	5.56E-06	0.0048 (0.026)
Silty Clay Loam	1.94E-05	0.017 (0.046)
Sand	8.25E-03	7.1 (3.7)
Sandy Clay	3.33E-05	0.029 (0.067)
Sandy Clay Loam	3.64E-04	0.31 (0.66)
Sandy Loam	1.23E-03	1.1 (1.4)

Table C-3. Total Porosity of Natural Porous Media.

(Bear, 1972)			(Freeze and Cherry, 1978)	
Sedimentary Materials/ Soil Type	Porosity Value in %		Unconsolidated Deposits	Porosity Value in %
Peat Soils	60-80		Gravel	25-40
Soils	50-60		Sand	25-50
Clay	45-55		Silt	35-50
Silt	40-50		Clay	40-70
Medium to Coarse Mixed Sands	35-40		Rocks	
Uniform Sand	30-40		Fractured Basalt	5-50
Fine to Medium Mixed Sands	30-35		Karst Limestone	5-50
Gravel	30-40		Sandstone	5-30
Gravel and Sand	30-35		Limestone Dolomite	0-20
Sandstone	10-20		Shale	0-10
Shale	1-10		Fractured Crystalline Rock	0-10
Limestone	1-10		Dense Crystalline Rock	0-5

Table C-4. Average Porosity (Standard Deviation) Values Based on Soil Texture.

	Porosity
Soil Type	(*n*)
Clay	0.38 (0.09)
Clay Loam	0.41 (0.09)
Loam	0.43 (0.10)
Loamy Sand	0.41 (0.09)
Silt	0.46 (0.11)
Silt Loam	0.45 (0.08)
Silty Clay	0.36 (0.07)
Silty Clay Loam	0.43 (0.07)
Sand	0.43 (0.06)
Sandy Clay	0.38 (0.05)
Sandy Clay Loam	0.39 (0.07)
Sandy Loam	0.41 (0.09)

Table C-5. Descriptive Statistics from Carsel & Parrish (1988) Data Set Tabulated Values: Mean (Standard Deviation).

Soil Type	Residual Saturation, S_{wr}	Bubbling Pressure Head, Ψ_b	Pore Size Distribution Index, λ
Clay	0.18 (0.089)	1.25 (1.88)	0.09 (0.09)
Clay Loam	0.23 (0.024)	0.53 (0.42)	0.31 (0.09)
Loam	0.18 (0.030)	0.28 (0.16)	0.56 (0.11)
Loamy Sand	0.14 (0.037)	0.081 (0.028)	1.28 (0.27)
Silt	0.074 (0.022)	0.62 (0.27)	0.37 (0.05)
Silty Loam	0.15 (0.033)	0.50 (0.30)	0.41 (0.12)
Silty Clay	0.19 (0.064)	2.0 (2.0)	0.09 (0.06)
Silty Clay Loam	0.21 (0.021)	1.0 (0.6)	0.23 (0.06)
Sand	0.10 (0.023)	0.069 (0.014)	1.68 (0.29)
Sandy Clay	0.26 (0.034)	0.37 (0.23)	0.23 (0.19)
Sandy Clay Loam	0.26 (0.015)	0.17 (0.11)	0.48 (0.13)
Sandy Loam	0.16 (0.041)	0.13 (0.066)	0.89 (0.17)

* Carsel and Parrish (1998) report mean and standard deviation of van Genuchten's 'α' parameter. Using Eq. (3.4.6) and a first-order expansion, the standard deviation of Ψ_b is approximated by.

$$\sigma \Psi_b \cong \frac{\sigma_\alpha}{\alpha^{-2}}$$

Table C-6. Brooks and Corey Soil Parameters from Carsel and Parrish (1988)
Example Values Converted to van Genuchten Capillary Parameters in LNAST Utility.

Soil Texture	Porosity n	Irreducible Water Saturation, S_{wr}	Displacement Pressure Head (m) Ψ_{baw}	Pore Size Distribution Index λ
Sand	0.43	0.105	0.045	1.13
Loamy Sand	0.41	0.139	0.051	0.908
Sandy Loam	0.41	0.159	0.083	0.685
Sandy Clay Loam	0.39	0.256	0.114	0.423
Loam	0.43	0.181	0.181	0.479
Sandy Clay	0.38	0.263	0.317	0.224
Silt Loam	0.45	0.149	0.353	0.372
Clay Loam	0.41	0.232	0.407	0.293
Silt	0.46	0.074	0.455	0.341
Silty Clay Loam	0.43	0.207	0.855	0.225
Clay	0.38	0.179	1.244	0.09
Silty Clay	0.36	0.194	1.990	0.09

LNAPL PHYSICAL PROPERTIES

Source:

Charbeneau, Randall (1997). Free Product Recovery of Petroleum Hydrocarbon Liquids, prepared for American Petroleum Institute.

Table C-7. Representative LNAPL Density Values (gm/cm^3).

Fluid Type	Temp. 0ºC	Source	Temp. 15ºC	Source	Temp. 20ºC	Source	Temp. 25ºC	Source
Water	1.000	C	0.998	C	0.998	C	0.996	C
Automotive Gasoline	0.746	A	0.729	A				
Automotive Diesel	0.838	A	0.827	A				
Kerosene	0.842	A	0.839	A			0.835	A
Jet Fuel (JP-3)			0.844	A	0.800	B		
Jet Fuel (JP-5)					0.820	B		
Fuel Oil #2	0.874	A	0.866	A	0.840	A		
Fuel Oil #4	0.914	A	0.904	A	0.900	B	0.898	A
Fuel Oil #5	0.932	A	0.923	A			0.917	A
Fuel Oil #6 or Bunker C	0.986	A	0.974	A			0.964	A
Electrical Lubricating Oil	0.882	A	0.974	A				
Electrical Lubricating Oil-used	0.883	A	0.874	A				
Electrical Insulating Oil	0.892	A	0.882	A				
Electrical Insulating Oil-used	0.878	A	0.867	A				
Norman Wells Crude	0.845	A	0.832	A			0.829	A
Avalon Crude	0.846	A	0.839	A			0.834	A
Alberta Crude	0.850	A	0.840	A			0.832	A
Transmountain Blend Crude	0.865	A	0.855	A				
Bow River Blend Crude	0.900	A	0.893	A			0.885	A
Prudhoe Bay Crude	0.915	A	0.905	A			0.900	A
Atkinson Crude	0.922	A	0.911	A			0.905	A
La Rosa Crude	0.923	A	0.914	A			0.908	A

Source: A-API, 1996; B-Mercer and Cohen, 1990; C-Vennard and Street, 1982.

Table C-8. Interfacial and Surface Tension (dynes/cm) at 20°C.

Chemical Name	Interfacial Tension	Surface Tension
Benzene	35	28.9
Ethylbenzene	35.5	29.3
Toulene	36.1	28.5
o-Xylene	36.1	30.3
Crude Oil	no data	24-38
Diesel Fuel	50	25
Gasoline	50	21
Naptha (BTX mixture)	45	20
Fuel Oil No. 1	48	27
Jet Fuel JP-4/5	50	25
Petroleum Distillates	50	21

Source: Mercer and Cohen (1990)

Note: Field experience strongly suggests that the oil/water interfacial tension is often much smaller than the laboratory based values in the table. Lower oil/water IFT implies a greater LNAPL saturation for the same capillary head condition. Since the IFT is used to scale exponential capillary parameters, it is suggested that literature values be used with caution. Measurements based on field samples is always preferred.

Table C-9. Representative Dynamic Viscosity Values (centipoise).

Fluid Type	Temp. 0 °C	Source	Temp. 15 °C	Source	Temp. 20 °C	Source	Temp. 25°C	Source
Water	1.79	B	1.14	B	1.00	B	0.89	B
Automotive Gasoline	0.75	A	0.62	A				
Automotive Diesel	3.90	A	2.70	A				
Kerosene	3.40	A	2.30	A			2.20	A
Jet Fuel (JP-3)								
Jet Fuel (JP-5)								
Fuel Oil #2	7.74	A			4.04	A		
Fuel Oil #4			47.2	A	22.7	A		
Fuel Oil #5			215	A			122	A
Fuel Oil #6 or Bunker C	7.0E+07	A					3180	A
Electrical Lubricating Oil	350	A	144	A				
Electrical Insulating Oil	37.8	A	18.8	A				
Norman Wells Crude	8.76	A	5.05	A			3.93	A
Avalon Crude	575	A	11.4	A			25.6	A
Alberta Crude	17.6	A	6.43	A			4.22	A
Transmountain Blend Crude	650	A	10.5	A				
Bow River Blend Crude	88.4	A	33.7	A			23.7	A
Prudhoe Bay Crude	577	A	68.4	A			35.3	A
Atkinson Crude	136	A	57.3	A			35	A
La Rosa Crude	640	A	180	A			104	A

Source: A-API, 1996; B-Vennard and Street, 1982.

LNAPL CHEMICAL PROPERTIES

Source:

American Petroleum Institute (1994). *Transport and Fate of Non-BTEX Petroleum Chemicals in Soils and Groundwater*, Health and Sciences Department, API Publication Number 4593, Washington, DC.

Table C-10. Concentrations of normal, branched, and cyclic alkanes in U.S. crude oils. Concentrations are in mg/l. From Speight (1991) (Page 1 of 2).

Compound	Ponca	n-Alkane Isoalkane	Santa Barbara	n-Alkane Isoalkane
Hexanes		2.2		0.76
n-hexane	18,000		7,230	
2-methylpentane	4,000		3,470	
3-methylpentane	3,000		4,180	
2,2-dimethylbutane	400		430	
2,3-dimethylbutane	800		1,400	
Heptanes		1.7		1.01
n-heptane	23,000		8,460	
3-methylhexane	5,000		1,880	
3-ethylpentane	500		--	
2-methylhexane	7,000		--	
2,3-dimethylpentane	1,000		6,010	
2,4-dimethylpentane	--		490	
Octanes		6.9		2.5
n-Octane	19,000		9,230	
2-methylheptane	--		--	
2,2-dimethylhexane	100		1,180	
2,3-dimethylhexane	600		1,630	
2,4-simethylhexane	600		--	
2,5-dimethylhexane	600		950	
3,3-dimethylhexane	300		--	
2-methyl-3-ethylpentane	400		--	
2,2,3-trimethylpentane	40		--	
2,3,3-trimethylpentane	60		--	
2,3,4-trimethylpentane	50		--	
Nonanes		2.6		0.87
n-nonane	18,000		5,800	
2-methyloctane	4,000		--	
3-methyloctane	1,000		4,200	
4-methyloctane	1,000		--	
2,3-dimethylheptane	500		--	

Table C-10. Concentrations of normal, branched, and cyclic alkanes in U.S. crude oils. Concentrations are in mg/l. From Speight (1991). (Page 2 of 2).

Compound	Ponca	Santa Barbara
Higher n-paraffins		
n-decane	18,000	--
n-undecane	17,000	--
n-dodecane	17,000	--
Cycloparaffins		
cyclopentane	500	460
methylcyclopentane	9,000	3,030
cyclohexane	7,000	--
ethylcyclopentane	2,000	1,860
1,1-dimethylcyclopentane	2,000	630
1-t-2-dimethylcyclopentane	5,000	1,540
1-c-3-dimethylcyclopentane	2,000	--
1-t-3-dimethylcyclopentane	9,000	2,380
propylcyclopentane	--	--
ethylcyclohexane	2,000	--
1-t-2-dimethylcyclohexane	--	2,640
1-c-3-dimethylcyclohexane	--	--
1,1,3-trimethylcyclopentane	3,000	--
1-t-2-c-trimethylcyclopentane	3,000	3,600
1-t-2-c-4-trimethylcyclopentane	2,000	--
1,1,2-trimethylcyclopentane	600	--
1,1,3-trimethylcyclopentane	2,000	--
1-t-2-t-4-trimethylcyclohexane	2,000	--

Table C-11. Concentrations of benzenes and naphthalenes in U.S. crude oils. Concentrations are in mg/kg. From Speight (1991).

Compound	Ponca	Santa Barbara	East Texas	Bradford	Greendale	Winkler	Midway	Conroe
benzene	2,000	2,210	700	600	2,100	400	700	4,100
toluene	5,000	7,780	5,800	5,100	5,900	900	4,300	24,600
ethylbenzene	2,000	2,090	2,200	900	1,200	800	2,200	3,100
o-xylene	3,000	2,900	3,000	2,100	1,700	300	3,100	6,800
m-xylene	5,000	--	6,400	6,100	4,000	800	3,600	20,300
p-xylene	1,000	6,800	1,700	1,700	900	1,200	1,500	5,900
n-propylbenzene	900	2,600	800	500	300	200	400	1,200
isopropylbenzene	700	600	400	300	300	300	300	900
1-methyl-2-ethylbenzene	900	--	700	300	400	100	300	900
1-methyl-3-ethylbenzene	1,700	--	1,600	1,300	800	100	400	4,000
1-methyl-4-ethylbenzene	600	--	700	500	300	500	300	1,300
1,2,3-trimethylbenzene	1,000	--	--	--	--	--	--	--
1,2,4-trimethylbenzene	5,100	--	3,400	3,300	1,500	1,300	1,300	6,900
1,3,5-trimethylbenzene	1,200	1,800	900	1,700	500	500	500	3,600
t-butylbenzene	100	--	100	20	30	20	0	100
1,2,3,4-tetramethylbenzene	2,000							
tetrahydronaphthalene	300							
naphthalene	600							
1-methylnaphthalene	1,000							
2-methylnaphthalene	2,000							
5-methyltetrahydronaphthalene	800							
6-methyltetrahydronaphthalene	900							

Table C-12. Concentrations of aromatic hydrocarbons in crude oils. Concentrations are in mg/kg. (Page 1 of 2).

Compound	S.Louisiana[1]	Kuwait[1]	Prudhoe Bay[2]	North Slope[3]	VMI Crude[4]	Wyoming Crude[5]
C_3-C_6 benzenes						8,100
tetralins						2,400
toluene			820			
ethylbenzene			560			
xylenes			2,840			
trimethylbenzenes			2,140			
indane			670			nd
C_2-C_4 indanes						800
tetramethylbenzenes			1,400			
naphthalene			920	210	326	900
C_1-C_3 naphthalenes						17,500
methylnaphthalenes			4,300	770	1,663	
dimethlynaphthalenes			3,980	1,400	3,142	
trimethylnaphthalenes			510	870	1,899	
tetramethylnaphthalenes				500	994	
biphenyl				63		400
C_1-C_3 biphenyls						2,200
fluorene				30	72	600
C_1-C_2 fluorenes						1,000
methylfluorenes				110	264	
dimethylfluorenes				160	435	
trimethylfluorenes				190	389	
phenanthrene	70	26	380	91	189	500
C_1-C_2 phenanthrenes						700
methylphenanthrenes	255	89	540	460	635	
dimethylphenanthrenes			110	790	825	
trimethylphenanthrenes				540	631	
tetramethylphenanthrenes				280	217	
dibenzothiophene				80	271	
methyldibenzothiophenes				150	849	
dimethyldibenzothiophenes				220	732	
trimethyldibenzothiophenes				190	888	
tetramethyldibenzothiophenes					309	
fluoranthene	5.0	2.9		nd	3.0	
pyrene	3.5	4.5		3.4	4.0	
methylfluoranthenes/ pyrenes				46	35	
benz(a)anthracene	1.7	2.3		nd	2.0	

Table C-12. Concentrations of aromatic hydrocarbons in crude oils. Concentrations are in mg/kg. (Page 2 of 2).

Compound	S.Louisiana[1]	Kuwait[1]	Prudhoe Bay[2]	North Slope[3]	VMI Crude[4]	Wyoming Crude[5]
methyl/dimethyl-benzanthracene					nd	
chrysene	18	6.9		16	14	
methylchrysenes				23	26	
dimethylchrysenes				32	47	
trimethylchrysenes				30		
triphenylene	10	2.8				
benzofluoranthenes	1.0	<1.0		2.0		
benzo(a)pyrene	0.75	2.8		nd		
benzo(e)pyrene	2.5	0.5		4.9		
perylene	34.8	<0.1		nd		
benzo(ghi)perylene	1.6	<1.0		nd		

(1) Pancirov and Brown, 1975
(2) Riley et al., 1981
(3) A.D. Little, 1991
(4) Burns et al., 1991
(5) Woodward et al., 1981

Table C-13. Concentrations of alkylbenzenes, selected polycyclic aromatic hydrocarbons, and dibenzothiophenes in crude oils. Concentrations are in mg/kg.

Compound	Alberta Sweet[1]	Mega Borg[2]	Handil Crudes[3]
alkylbenzenes		600	
naphthalene	382		
methylnaphthalenes		1092	4860
ethylnaphthalenes			960
dimethylnaphthalenes		1428	9480
trimethylnaphthalenes		924	5100
tetramethylnaphthalenes	336		
acenaphthylene	13		
acenaphthene	57		
fluorene	59	66	
methylfluorenes	150	150	
dimethylfluorenes		228	
trimethylfluorenes		156	
phenanthrene	150	252	258
methylphenanthrenes	370	420	578
dimethylphenanthrenes	500	304	372
trimethylphenanthrenes		63	
dibenzothiophene		63	
methyldibenzothiophenes	143		
dimethyldibenzothiophenes		155	
trimethyldibenzothiophenes		63	
anthracene	11		
fluoranthene	6.0		
pyrene	17		
methylpyrene	39		
chrysene	30		
benzo(b)fluoranthene	4.0		
benzo(e)pyrene	5.0		
benzo(a)pyrene	nd		
methylcholanthrene	3.0		

(1) Benner et al., 1990
(2) Fawn and Barker, 1991
(3) Radke et al., 1990

Table C-14. Concentrations of PAH and heterocyclic compounds in a sample of Qatar crude oil. Concentrations are mg/kg. Numbers in parentheses are number of isomers quantified. From Grimmer et al. (1983).

Aromatics		Heterocyclics	
Compound	**Concentration**	**Compound**	**Concentration**
phenanthrene	>128.7	dibenzothiophene	>336.5
3-methylphenanthrene	>17.2	4-methyldibenzothiophene	>6.7
2-methylphenanthrene	>12.7	2-methyldibenzotheophene	>21.4
9-methylphenanthrene	>33.4	3-methyldibenzothiophene	>0.2
1-methylphenanthrene	>20.9	1-methyldibenzothiophene	>0.6
1-phenylnaphthalene	>0.1	C_2-carbazoles (6)	>2.7
fluoranthene	1.7	dimethdibenzotheophene	>3.5
pyrene	10.7	dimethylxanthene	>0.4
benzo(a)fluorene	10.8	C_3-carbazoles (8)	36.5
benzo(b&c)fluorenes	6.2	C_4-carbazoles (8)	56.5
4-methylpyrene	11.6	C_5-carbazoles (9)	49.8
1-methylpyrene	22.9	methylphenanthrothiophene	2.2
benzo(c)phenanthrene	0.4	C_6-carbazoles (9)	45.3
benz(a)anthracene	6.7	benzonaphthothiophene	122.3
chrysene/triphenyline	43.5	methylbenzonaphthothiophenes	200.4
3-methylchrysene	43.9	dimethylbenzonaphthothiophenes	9.8
2-methylchrysene	24.5	methylfuran derivatives (3)	13.6
4-/6-methylchrysene	15.6	thiophene derivative	39.2
other methylchrysenes (3)	27.6	triphenylene (4,4a,4b,5-bcd)-thiophene	6.2
dimethylchrysenes (8)	82.9	methylthiophene derivatives (9)	107.7
benzo(b&j)fluoranthenes	7.4	thiophene derivative	11.0
benzo(k)fluoranthene	15.9	methylfuran derivative	1.2
benzo(e)pyrene	28.9	methylthiophene derivatives (10)	30.7
benzo(a)pyrene	3.6	dithiophene derivatives (9)	13.7
methylbenzofluoranthenes (7)	58.0	sulfur-substituted PAHs (2)	6.3
dimethylbenzofluoranthenes (12)	27.2	methylfuran derivative	11.9
indeno(1,2,3-cd)pyrene	7.4	methylated sulfur-substituted PAHs (4)	13.7
benzo(ghi)perylene	5.0		
methylpicines (2)	6.4		
methylindeno(1,2,3-cd) pyrenes (2)	4.5		
coronene	0.3		

Table C-15. Concentrations of sulfur-substituted alkanes in Wasson, Texas crude oil. Concentrations are in mg/l. From Speight (1991).

Compound	Wasson Crude
methanethiol	24
ethanethiol	53
2-thiapropane	8.8
2-propanethiol	19.9
2-methyl-2-propanethiol	5.5
2-thiabutane	22.2
1-propanethiol	4.1
3-methyl-2-thiabutane	6.4
2-butanethiol	38.6
2-methyl-1-propanethiol	0.3
3-thiapentane	7.5
2-thaipentane	3.0
1-butanethiol	trace
2-methyl-2-butanethiol	6.4
2-pentanethiol	14.0
3-pentanethiol	5.7
3-thiahexane	1.2
2,4-dimethyl-3-thiapentane	5.3
2,2-dimethyl-3-thiapentane	0.58
thiacyclopentane	0.77
2-thiahexane	0.77
2-methyl-3-thiahexane	0.78
2-methylthiacyclopentane	23
4-methyl-3-thiahexane	5.0
3-methyltiacyclopentane	4.6
2-hexanethiol	28
thiacyclohexane	3.2
t-2,2-dimethylthiacyclopentane	25
c-2,5-dimethylthiacyclopentane	24
3-thiapentane	0.78
2-methylthiacyclohexane	29
3-methylthiacyclohexane	0.24
4-methylthiacyclohexane	0.48
cyclohexanethiol	12

Table C-16. Variability in the concentrations of major aromatic components of 31 samples of leaded and unleaded gasoline from north and central Florida. From Cline et al. (1991).

Compound	Concentration (wt%)			
	Mean	Minimum	Maximum	Standard Deviation
benzene	1.73	0.7	3.8	0.68
toluene	9.51	4.5	21.0	3.59
ethylbenzene	1.61	0.7	2.8	0.48
m-,p-xylenes	5.95	3.7	14.5	2.07
o-xylene	2.33	1.1	3.7	0.72
n-propylbenzene	0.57	0.13	0.85	0.14
3,4-ethyltoluene	2.20	1.5	3.2	0.40
1,2,3-trimethylbenzene	0.8	0.6	1.1	0.12

Table C-17. Concentrations of alkanes, olefins, aromatic hydrocarbons, and additives in gasolines. Concentrations in volume or weight percent, except as indicated. (Page 1 of 3).

Compound	PS-6[1]	Unleaded[2]	Leaded[2]	1974 Gasoline[3]	IARC[4]	36-117 US Cut[5]
n-alkanes						
butane	3.83	4-5	4-5		3-12	
pentane	3.11	2.6-2.7	2.6-2.7		1-9	
hexane	1.58				<1-6	
C_7-C_{10}-n-alkanes	1.21				<1-5	
Isoalkanes						
isobutane	1.14					
isopentane	8.72	9-11	9-11		5-10	
methhylpentanes	6.29				4-19	
2,3-dimethylbutane	1.66				<1-2	
C_6-isoalkanes	0.18					
dimethylpentane					<1-7	
methylhexanes	2.38					
dimethylhexanes	2.16					
C_7-isoalkanes	0.23					
trimethylpentanes	11.74				<1-14	
C_8-isoalkanes	4.98					
methyloctanes	1.51					
C_9-isoalkanes	0.50					
C_{10}-C_{13}-isoalkanes	2.65					
Cycloalkanes						
cyclopentane	0.15					1.13
methylcyclopentane	0.97				<1-3	7.27
ethylcyclopentane						2.92
trimethylcyclopentane						5.31
cyclohexane	0.08				<1-3	8.39
dimethylcyclopentane	0.77					
methylcyclohexane					<1-7	18.2
C_7-cycloalkanes	0.32					
C_8-cycloalkanes	0.74					
C_9-cycloalkanes	1.03					
C_{10}-C_{13}-cycloalkanes	0.62					

Table C-18. Concentrations of alkanes, olefins, aromatic hydrocarbons, and additives in gasolines. Concentrations in volume or weight percent, except as indicated. (Page 2 of 3).

Compound	PS-6[1]	Unleaded[2]	Leaded[2]	1974 Gasoline[3]	IARC[4]	36-117 US Cut[5]
Mono-olefins		5	10			
propylene	0.03					
butene	0.75					
C_4-alkenes	0.15					
methylbutenes					<1-4	
pentenes	1.22				<1-2	
C_5-alkenes	0.07					
C_6-alkenes	0.14					
methylpentenes	1.26					
C_7-C_{12}-alkenes	5.34					
Aromatics						
benzene	1.94	0.7-3.8	2-5		<1-4	3.03
toluene	4.73	4.5-21	6-7		5-22	12.05
ethylbenzene	2.00	0.7-2.8	5		<1-2	
o-xylene	2.27	1.1-3.7			1-10	
m-xylene	5.66	3.7-14.5				
p-xylene	1.72	"				
n-propylbenzene		0.13-0.85				
methylethylbenzenes	3.10	1.5-3.2			<1-2	
trimethylbenzene	3.26	0.6-1.1				
C_9-alkylbenzenes	2.51					
C_{10}-alkylbenzenes	2.21					
C_{11}-alkylbenzenes	0.57					
C_{12}-alkylbenzenes	0.21					
C_9-C_{13}-indans/ tetralins	1.59					
naphthalene		0.2-0.5	0.2-0.5			
C_{10}-C_{12}-naphthalenes	0.74					
anthracene		1.8 mg/l	1.8 mg/l			
fluoranthene				6.5 mg/l		
pyrene				4.4 mg/l		
benz(a)anthracene				4.3 mg/l		
chrysene				2.0 mg/l		
benzo(b)fluoranthene		3.9 mg/l	3.9 mg/l			
benzo(e)pyrene			0.8 mg/l			

Table C-18. Concentrations of alkanes, olefins, aromatic hydrocarbons, and additives in gasolines. Concentrations in volume or weight percent, except as indicated. (Page 3 of 3).

Compound	PS-6[1]	Unleaded[2]	Leaded[2]	1974 Gasoline[3]	IARC[4]	36-117 US Cut[5]
Aromatics (continued)						
benzo(a)pyrene				1.8 mg/l		
benzo(ghi)perylene				2.2 mg/l		
coronene				1.1 mg/l		
Nonhydrocarbons						
tetraethyllead			600 mg/l			
tetramethyllead		5 mg/l				
dichloroethane		210 mg/l				
dibromomethane			190 mg/l			
methyl *tert*butyl ether		to 15%			<1-4	

(1) Barker et al., 1991
(2) Cline et al., 1991
(3) Guerin, 1977
(4) IARC, 1989
(5) Nyer and Skladany, 1989

Table C-19. Variability in composition of gasolines from Houston, TX area in 1984. Concentrations are weight percent. From Diakun (1984). (Page 1 of 2).

Compound	Regular Blend	Lead-Free Blend	Super Unleaded	API Generic
Alkanes				
propane	0.10	0.04	0.04	0.07
iso-butane	0.59	0.77	0.90	0.75
n-butane	4.31	4.41	3.42	4.50
iso-pentane	7.77	10.13	8.02	9.25
n-pentane	5.05	5.09	1.94	4.91
2,2-dimethylbutane	0.61	0.41	0.10	0.48
cyclopentane	0.87	0.52	0.18	0.66
2,3-dimethylbutane	1.18	1.04	0.92	1.14
MTBE*	0.12	0.25	2.02	0.42
2-methylpentane	5.44	3.97	2.01	4.59
3-methylpentane	3.52	2.44	1.22	2.90
n-heptane	3.91	1.92	0.72	2.79
methylcyclopentane	2.10	1.48	0.82	1.74
2,2-dimethylpentane	0.52	0.56	0.72	0.59
cyclohexane	0.44	0.17	0.07	0.29
2-methylhexane	2.59	2.12	1.58	2.34
2,3-dimethylpentane	0.06	0.04	0.06	0.05
3-methylhexane	2.07	1.57	0.94	1.77
1-cis-3-dimethylcyclopentane	0.39	0.34	0.21	0.36
1-trans-3-dimethylcyclopentane	0.34	0.30	0.18	0.32
3-ethylpentane	0.54	0.40	0.25	0.46
2,2,4-trimethylpentane	1.21	2.43	5.02	2.26
n-heptane	1.42	0.91	0.51	1.12
methylcyclohexane	0.91	0.70	0.43	0.77
ethylcyclopentane	0.22	0.20	0.12	0.21
2,5-dimethylhexane	0.43	0.60	0.98	0.58
2,4-dimethylhexane	0.37	0.45	0.64	0.45
3,3-dimethylhexane	0.57	1.08	1.98	1.06
2,3-dimethylhexane	0.34	0.35	0.53	0.36
2-methylheptane	0.67	0.57	0.45	0.60
3-methylheptane	0.74	0.66	0.49	0.67
2,2,5-trimethylhexane	0.28	0.37	0.67	0.37
n-octane	0.62	0.49	0.41	0.54
n-nonane	0.36	0.22	0.17	0.28
n-decane	0.24	0.14	0.09	0.17
n-undecane	0.34	0.32	0.30	0.32
n-dodecane	0.19	0.12	0.07	0.13
C_{11}-C_{12}	3.21	2.38	1.97	2.13
C_{12} plus	1.21	2.12	1.37	0.92

Table C-19. Variability in composition of gasolines from Houston, TX area in 1984. Concentrations are weight percent. From Diakun (1984). (Page 2 of 2).

Compound	Regular Blend	Lead-Free Blend	Super Unleaded	API Generic
Olefins				
propylene	0.01	0.01	0.02	0.01
isobutylene	0.10	0.10	0.11	0.11
1-butene	0.14	0.20	0.27	0.19
trans-2-butene	0.28	0.38	0.45	0.37
cis-2-butene	0.28	0.35	0.39	0.34
3-methyl-1-butene	0.11	0.13	0.10	0.12
1-pentene	0.40	0.44	0.33	0.43
2-methyl-1-butene	0.63	0.75	0.58	0.71
isoprene	0.03	0.03	0.03	0.03
trans-2-pentene	0.98	1.05	0.90	1.05
cis-2-pentene	0.50	0.52	0.44	0.52
2-methyl-2-butene	1.14	1.19	1.06	1.21
trans-1,3-pentadiene	0.04	0.04	0.03	0.04
cyctopentadiene	0.02	0.02	0.03	0.02
cis-1,3-pentadiene	0.02	0.02	0.01	0.02
cyclopentene	0.21	0.21	0.24	0.22
3-methyl-1-pentene	0.12	0.12	0.09	0.12
4-methyl-2-pentene	0.13	0.12	0.10	0.13
2-methyl-1-pentene	0.23	0.21	0.17	0.22
1-hexene	0.16	0.15	0.11	0.15
C_6-olefins	1.85	1.67	1.68	1.84
1-methylcyclopentene	0.14	0.09	0.05	0.11
1-octene	0.14	0.12	0.08	0.12
1-nonene	0.04	0.09	0.01	0.10
1-decene	0.03	--	0.01	0.01
1-undecene	--	0.02	0.01	--
1-dodecene	0.22	0.13	0.10	0.14
Aromatics				
benzene	1.80	1.92	1.42	1.79
toluene	5.46	7.77	15.87	7.92
ethylbenzene	1.52	1.96	2.45	1.83
p- and m-xylenes	4.45	5.82	7.18	5.38
o-xylene	1.68	2.23	2.82	2.06
isopropylbenzene	0.16	0.18	0.27	0.17
n-propylbenzene	0.51	0.64	0.75	0.61
1-methyl-3-ethylbenzene	1.93	2.19	2.36	2.05

Table C-20. Typical hydrocarbon composition of three grades of jet fuel. Concentrations are in weight percent. From Smith et al., (1981). (Page 1 of 3).

Compound	JP-4	JP-5	JP-8
n-alkanes			
butane	0.12	--	--
pentane	1.06	--	--
hexane	2.21	--	--
heptane	3.67	--	0.03
octane	3.80	0.12	0.09
nonane	2.25	0.38	0.31
decane	2.16	1.79	1.31
undecane	2.32	3.95	4.13
dodecane	2.00	3.94	4.72
tridecane	1.52	3.45	4.43
tetradecane	0.73	2.72	2.99
pentadecane	--	1.67	1.61
hexadecane	--	1.07	0.45
heptadecane	--	0.12	0.08
octadecane	--	--	0.02
isoalkanes			
isobutane	0.66	--	--
2,2-dimethylbutane	0.10	--	--
2-methylpentane	1.28	--	--
3-methylpentane	0.89	--	--
2,2-dimethylpentane	0.25	--	--
2-methylhexane	2.35	--	--
3-methylhexane	1.97	--	--
2,2,3,3-tetramethylbutane	0.24	--	--
2,5-dimethylhexane	0.37	--	--
2,4-dimethylhexane	0.58	--	--
3,3-dimethylhexane	0.26	--	--
2,2-dimethylhexane	0.71	--	--
2-methylheptane	2.70	--	--
4-methylheptane	0.92	--	--
3-methylheptane	3.04	--	--
2,5-dimethylheptane	0.52	--	--
2,4-dimethylheptane	0.43	--	--
4-ethylheptane	0.18	--	--
4-methyloctane	0.86	--	--
2-methyloctane	0.88	--	--

Table C-20. Typical hydrocarbon composition of three grades of jet fuel. Concentrations are in weight percent. From Smith et al., (1981). (Page 2 of 3).

Compound	JP-4	JP-5	JP-8
isoalkanes, continued			
3-methyloctane	0.79	0.07	0.04
2-methylundecane	0.64	--	--
2,6-dimethylundecane	0.71	--	--
2,4,6-trimethylheptane	--	0.07	0.07
4-methyldecane	--	0.78	--
2-methyldecane	--	0.61	0.41
2,6-dimethyldecane	--	0.72	0.66
2-methylundecane	--	1.39	1.16
2,6-dimethylundecane	--	2.00	2.06
cycloparaffins			
methylcyclopentane	1.16	--	--
cyclohexane	1.24	--	--
t-1,3-dimethylcyclopentane	0.36	--	--
c-1,3-dimethylcyclopentane	0.34	--	--
c-1,2-dimethylcyclopentane	0.54	--	--
methylcyclohexane	2.27	--	--
ethylcyclopentane	0.26	--	--
1,2,4-trimethylcyclopentane	0.25	--	--
1,2,3-trimethylcyclopentane	0.25	--	--
c-1,3-dimethylcyclohexane	0.42	--	--
1-methyl-3-ethylcyclohexane	0.17	--	--
1-methyl-2-ethylcyclohexane	0.39	--	--
dimethylcyclohexane	0.43	--	--
1,3,5-trimethylcyclohexane	0.99	0.09	0.06
1,1,3-trimethylcyclohexane	0.48	0.05	0.06
1-methyl-4-ethylcyclohexane	0.48	--	0.10
n-butylcyclohexane	0.70	0.90	0.74
propylcyclohexane	--	--	0.14
hexylcyclohexane	--	--	0.93
heptylcyclohexane	--	0.99	1.00
aromatic hydrocarbons			
benzene	0.50	--	--
toluene	1.33	--	--
ethylbenzene	0.37	--	--

Table C-20. Typical hydrocarbon composition of three grades of jet fuel. Concentrations are in weight percent. From Smith et al., (1981). (Page 3 of 3).

Compound	JP-4	JP-5	JP-8
aromatic hydrocarbons, continued			
m-xylene	0.96	0.13	0.06
p-xylene	0.35	--	--
o-xylene	1.01	0.09	0.06
isopropylbenzene	0.30	--	--
n-propylbenzene	0.71	--	--
1-methyl-3-ethylbenzene	0.49	--	--
1-methyl-4-ethylbenzene	0.43	--	--
1,3,5-trimethylbenzene	0.42	--	--
1-methyl-2-ethylbenzene	0.23	--	--
1,2,4-trimethylbenzene	1.01	0.37	0.27
1,3-diethylbenzene	0.46	0.61	--
1,4-diethylbenzene	--	0.77	--
1-methyl-4-propylbenzene	0.40	--	--
1,3-dimethyl-5-ethylbenzene	0.61	--	0.62
1-methyl-2-isopropylbenzene	0.29	--	0.56
1,4-dimethyl-2-ethylbenzene	0.70	--	--
1,2-dimethyl-4-ethylbenzene	0.77	--	--
1,2,3,4-titramethylbenzene	0.75	1.48	1.12
1-ethylpropylbenzene	--	1.16	0.99
1,2,4-triethylbenzene	--	0.72	0.99
1,3,5-triethylbenzene	--	--	0.60
phenylcyclohexane	--	0.82	0.87
1-t-butyl-3,4,5-trimethylbenzene	--	0.24	--
n-heptylbenzene	--	0.27	0.25
naphthalene	0.50	0.57	1.14
2-methylnaphthalene	0.56	1.38	1.46
1-methylnaphthalene	0.78	1.44	1.84
2,6-dimethylnaphthalene	0.25	1.12	1.34
biphenyl	--	0.70	0.63
1-ethylnaphthalene	--	0.32	0.33
2,3-dimethylnaphthalene	--	0.46	0.36
n-octylbenzene	--	0.78	0.61
olefins			
tridecene	--	0.45	0.73

Table C-21. Hydrocarbon composition of two samples of kerosene. From Goodman and Harbison (198?). (Page 1 of 2).

Compound/Class	Sample A	Sample B
hydrocarbon type (vol %)		
paraffins	50.5	42.7
monocycloparaffins & olefins	25.3	19.3
dicycloparaffins	5.6	8.9
alkylbenzenes	12.7	14.7
indans/tetralins	2.9	7.5
naphthalene & alkylnaphthalenes	3.0	6.9
n-paraffins (wt %)		
heptane	0.1	0.1
octane	0.2	0.3
nonane	0.4	0.8
decane	1.5	1.7
undecane	3.5	6.1
dodecane	2.8	5.7
tridecane	3.1	5.2
tetradecane	2.3	4.7
pentadecane	0.6	2.3
hexadecane	0.1	0.7
heptadecane	--	0.4
octadecane	--	0.3
nonadecane	--	0.2
eicosane	--	0.1
heneicosane	--	0.1
aromatic hydrocarbons (ppm, wt/vol)		
indene	<50	2.2
naphthalene	2,000	1,286
1-methylnaphthalene	2,200	2,160
2-methylnaphthalene	2,100	2,860
acenaphthene	51	40
acenaphthalene	25	38
fluorene	<2.0	36
1,4-dimethylnaphthalene	1,200	1,580
phenanthrene	1.9	493

Table C-21. Hydrocarbon composition of two samples of kerosene. From Goodman and Harbison (198?). (Page 2 of 2).

Compound/Class	Sample A	Sample B
anthracene	<2.0	7.3
fluoranthene	<4.0	1.0
pyrene	<2.0	2.0
benz(a)anthracene	<0.75	<0.09
chrysene	<2.0	<0.11
benzo(b)fluoranthene	<0.75	<0.20
benzo(k)fluoranthene	<0.50	<0.04
benzo(a)pyrene	<0.50	<0.30
benzo(g,h,i)perylene	<2.0	<0.30
indeno(1,2,3-c,d)pyrene	<2.0	<0.30
perylene	<3.0	<0.90
dibenz(a,h)anthracene	<0.75	<0.50
dibenzo(def,p)chrysene	<0.30	<0.15
9,10-dimethylanthracene	<4.0	6.0
2-methylanthracene	<4.0	3.9
benzo(b)fluorene	<4.0	1.0
benzo(a)fluorene	<4.0	0.78
7,12-dimethylbenz(a)anthracene	--	17.0
dibenzo(a,e)pyrene	<0.45	<0.30
benzo(b)chrysene	<0.45	<0.30
picene	<1.5	<1.4
p-quarterphenyl	<0.5	<0.50
coronene	<0.45	<0.30
dibenz(a,h)acridine	<0.2	<0.13
dibenzo(a,h)pyrene	<1.0	<0.70
3-methylcholanthrene	<0.1	<0.08
benzo(g,h,i)fluoranthene	<1.0	<0.04
naphtho(1,2,3,4,def)chrysene	<0.15	<0.10

Table C-22. Hydrocarbon composition of typical home heating oils. Concentrations are volume percent. From IARC (1989).

Hydrogen Type	Straight-run No. 1 Furnace Oils 1	Straight-run No. 1 Furnace Oils 2	Hydrotreated No. 1 Furnace Oil	Straight-run No. 2 Furnace Oil	No. 2 Furnace Oil 10% Calalytic	No. 2 Furnace Oil 50% Calalytic
n/iso-paraffins	50.5	54.3	42.6	41.3	61.2	57.2
monocycloparaffins	25.3	18.4	19.3	22.1	8.5	6.0
bicycloparaffins	5.6	4.5	8.9	9.6	8.3	5.0
tricycloparaffins	--	0.8	--	2.3	1.4	0.7
total alkanes	81.4	78	70.9	75.3	79.4	68.9
olefins	--	--	--	--	2.0	7.5
alkylbenzenes	12.7	14.3	14.7	5.9	5.3	8.0
indans/tetralins	2.9	3.8	7.5	4.1	4.3	5.4
dinaphthenobenzenes/indenes	--	0.9	--	1.8	1.3	1.0
naphthalenes	3.0	2.6	6.9	8.2	5.8	6.8
biphenyls/acenaphthanes	--	0.4	--	2.6	1.1	1.6
fluorenes/acenaphthylenes	--	--	--	1.4	0.6	0.3
phenanthrenes	--	--	--	0.7	0.2	0.5
total aromatic hydrocarbons	18.6	29.1	22.0	24.7	18.6	23.6

Table C-23. Concentrations of benzenes and PAH in middle distillate fuels. Concentrations are in mg/kg.

Compound	No. 2 Fuel Oil[1]	Artic Diesel[2]	Refined Spilled[3]	Diesel Fuel[4]	No. 2 Heating[4]
benzene	222,000[a]	<10			
toluene		2,549			
ethylbenzene		991			
xylenes	5,211				
naphthalene	4,000	4,086[a]	2,468		
methylnaphthalenes	27,100		23,312		
ethylnaphthalenes			5,576		
dimethylnaphthalenes	31,100		26,214		
trimethyl-naphthalenes	18,400				
fluorene	3,600	302[a]			
anthracene				2.9	3.6
phenanthrene	429	171[a]			
methylanthracenes				9.3	15.7
methylphenanthrenes	7,850				
fluoranthene	37			0.57	2.4
pyrene	41			0.37	1.3
benz(a)anthracene	1.2			0.13	0.04
chrysene	2.2	<10[a]		0.45	0.54
triphenylene	1.4			3.3	0.73
benzo(a)pyrene	0.6			0.07	0.03
benzo(e)pyrene	0.1			0.18	0.02
benzo(g,h,i)perylene				0.03	0.03

(1) Pancirov and Brown, 1975
(2) Kennicutt et al., 1991
(3) Woodward et al., 1983
(4) Norris and Hill, 1974
(a) includes alkyl homologues

Table C-24. Concentrations of benzenes and PAH in No. 2 diesel fuels. Concentrations are in mg/l or mg/kg.

Compound	No. 2 Fuel Oil[1]	No. 2 Fuel Oil[2]	High S Diesel Fuel[2]	Low S Diesel Fuel[2]
toluene			8,300	nd
xylenes			200	2,700
trimethylbenzenes			27,000	17,000
C_4-benzenes			31,000	23,000
C_5-benzenes			13,000	11,000
C_6-benzenes			1,900	4,600
naphthalene	500	76	25,000	2,200
methylnaphthalenes	1,000	560	30,000	7,100
dimethylnaphthalenes	1,300	1,500	43,000	10,000
trimethylnaphthalenes	950	1,000	34,000	7,200
tetramethylnaphthalenes	550	520	1,200	900
biphenyl	75	52		
fluorene	38	40		
methylfluorenes	135	130		
dimethylfluorenes	305	240		
trimethylfluorenes	315	170		
phenanthrene	80	88	2,100	400
methylphenanthrenes	500	370	5,300	400
dimethylphenanthrenes	950	470	4,300	200
trimethylphenanthrenes	700	190	1,500	nd
tetramethylphenenthrenes	285	76		
dibenzothiophene	nd	150		
methyldibenzothiophenes	22	65		
dimethyldibenzothiophenes	80	84		
trimethyldibenzothiophenes	90	62		
fluoranthene	2.8	1.2		
pyrene	20	7.0		
methylfluoranthenes/pyrenes	80	15		
benz(a)anthracene	0.8	0.12		
chrysene	3.4	0.5		
methylchrysenes	6.0	0.8		
diemthylchrysenes	3.7	0.4		
trimethylchrysenes	1.6	0.08		
benzo(a)pyrene	nd	0.13		
benzo(e)pyrene	nd	nd		
benzo(g,h,i)perylene	nd	0.05		

(1) Page et al., 1994

(2) Boehm et al., 1989

Table C-25. Concentrations of benzenes and PAH in residual petroleum products. Concentrations are in mg/l or mg/kg.

Compound	Bunker C No. 6 Oil[1]	Bunker C[2]	Asphalts[3]	Paving Asphalts[4]
benzenes	60,000[a]			
naphthalene	1,000			
methylnaphthalenes	7,500	1,700		
dimethylnaphthalenes	12,300	6,100		
trimethylnaphthalenes	8,800			
biphenyls	<100			
fluorenes	2,400			3.0
phenanthrene	482	1,700	0.4-3.5	9.6
methylphenenthrenes	871	3,300		
dimethylphenanthrenes		3,500		
fluoranthene	240		nd-5	
pyrene	23		0.08-38	
benz(a)anthracene	90		nd-35	90
chrysene	196		0.04-34	80
triphenylene	31		0.25-7.6	
dimethylbenzanthracenes				4.3
benzo(k)fluoranthene				1.8
benzo(a)pyrene	44		nd-27	1.3
benzo(e)pyrene	10		0.03-52	
perylene	22		nd-39	1.5
benzo(g,h,i)perylene			tr-15	1.2
dibenz(a,h)anthracene				4.6

(1) Pancirov and Brown, 1975
(2) Petersen, 1978
(3) Wallcave et al., 1971
(4) Malaiyandi et al., 1982

Table C-26. Concentrations of PAH in new engine oils and lube oil. Concentrations are in mg/kg.

Compound	Engine Oil (new)[1]	Average[1]	Maximum	Rerefined[1]	Lube Oil[2]
dibenzo(b,d)thiophene	5				
fluorene					11.7
phenanthrene	7				46.5
anthracene	0.1				9.5
methyldibenzothiophenes	1				
methylphenanthrenes	8				
fluoranthene	0.7	0.3	3	69 2.0	
phenanthrothiophene	0.4				
pyrene	2	0.7	7	12 2.5	
benzonaphthofurans	1				
methylpyrenes/ fluoranthenes	1				
benzofluorenes	4				
methylbenzonaphthofurans	0.3				
methylpyrenes	3				
dimethylpyrenes/ fluoranthenes	1				
benzonaphthothiophenes	5	1	9	5	
benz(a)anthracene	0.30.2	2			0.68
triphenylene	3				
chrysene	1	1	12	30	3.2
methylbenzonaphtho-thiophenes	7				
methylchrysenes	1				
dimethylchrysenes	1				
benzofluoranthenes	0.4	0.1	0.2	8 0.62	
triphenylenethiophene	0.1				
benzo(e)pyrene	0.25	0.2	0.4	4	
benzo(a)pyrene	0.03	0.06	0.3	1	0.23
methyltriphenylene/ thiophene	0.3				
methylbenzo(e)pyrenes	0.2				
methylbenzo(a)pyrenes	0.1				
dimethylbenzopyrenes	0.5				
indeno(1,2,3-c,d)pyrene	0.02	0.006	0.02	0.7	
dibenz(a)anthracene	0.1				
benzo(g,h,i)perylene	0.1	0.05	0.1	1	0.85
anthranthrene	0.01	0.03			
coronene		0.007	0.02	0.6	

(1) Grimmer et al., 1981a
(2) Eisenberg et al., 1988

Table C-27. Concentrations of alkylbenzenes and PAH in used engine oils from North America. Concentrations are in mg/l or mg/kg. (Page 1 of 2).

Compound	Winter Gas Engine Calgary[1]	Gas Engine 3928 mi[2]	Gas Engine 5817 mi	Waste Crankcase Oil (MD)[3]
Σ alkylbenzenes	>900			
tetralin				24
naphthalene	2,350	2,520	368	
methylnaphthalenes		6,350	4,150	57
dimethylnaphthalenes		4,470	3,000	114
trimethylnaphthalenes				37
Σ alkylnaphthalenes	440			
biphenyl		82.8	45.8	
methylbiphenyls	2.05			6
fluorene	1.47	98.3	109	6
methylfluorenes	2.45			
dimethylfluorenes	1.29			
trimethylfluorenes	1.10			
phenanthrene	7.80	186	193	33
anthracene	0.33	30.1	47.0	
phenylnaphthalene	0.90			
methylphenanthrenes	11.67	648	668	
dimethylphenanthrenes	10.59			
trimethylphenanthrenes	6.13			
diethylphenanthrenes	1.19			
ethylcyclopentaphenanthrene	1.42			
methylanthracenes	0.58			
dimethyanthracenes	0.26			
trimethylanthracenes	0.51			
dibenzothiophene	0.79			
methyldibenzothiophenes	2.26			
dimethyldibenzothiophenes	3.86			
trimethyldibenzothiophenes	1.94			
benzonaphthiophene	0.34			
methylbenzonaphthothiophene	0.54			
terphenyl	0.12			
fluoranthene	4.36	69.8	91.2	
pyrene	6.69	88.4	95.6	
methylpyrenes	4.25			
dimethylpyrenes	1.71			
ethylmethylpyrenes	0.14			
benzofluorenes	2.75			

Table C-27. Concentrations of alkylbenzenes and PAH in used engine oils from North America. Concentrations are in mg/l or mg/kg. (Page 2 of 2).

Compound	Winter Gas Engine Calgary[1]	Gas Engine 3928 mi[2]	Gas Engine 5817 mi	Waste Crankcase Oil (MD)[3]
benzo(c)phenanthrene	0.12			
benz(a)anthracene	0.87	32	47.4	
methylbenz(a)anthracene	2.45			
ethylbenz(a)anthracene	0.65			
chrysene/triphenylene	2.48	50	84.7	
cyclopenta(cd)pyrene	0.78			
benzo(b)fluoranthene	1.44			
methylbenzofluoranthenes	0.43			
benzo(e)pyrene	1.74	nd	27.1	
benzo(a)pyrene	0.36	nd	22.3	
methylbenzopyrenes	0.41			
perylene	0.13			
benzo(ghi)perylene	1.67			

(1) Peake and Parker, 1980
(2) Pruell and Quinn, 1988
(3) Hoffman et al., 1982

Table C-28. Concentrations of PAH in used engine oils (crankcase oils). Concentrations are in mg/kg. From Grimmer et al., (1981b).

Compound	Length of Use and Engine Type				
	610K km Gasoline	1-6K km Gasoline	0.5-6K km Diesel	3-30K km Diesel	9-31K Diesel
phenanthrene	158				
anthracene	46				
methylphenanthrenes	381				
2-phenylnaphthalene	44				
dimethylphenanthrenes (includes O-PAC)	56				
fluoranthene	178	109	59	3	3
pyrene	430	326	78	6	5
methylfluoranthenes /methylpyrenes	883				
dimethylfluoranthenes	263				
benz(a)anthracene	245				
benzo(b)naphtho-(2,1-d)thiophene			4	6	5
chrysene+triphenylene	223	74	43	6	8
methylchrysenes/ benz(a)anthracenes	485				
dimethylbenz(a)anthracene	21				
benzo(b+j)fluoranthenes	134	44	17	1	1
benzo(k)fluoranthene	37				
benzo(a)fluoranthene	19				
benzo(e)pyrene	278	49	11	1	1
benzo(a)pyrene	217	35	12	0.6	0.6
perylene	51	10	3	0.4	0.3
methylperylenes/ benzopyrenes/benzo-fluoranthenes	540				
dimethylperylenes/ benzopyrenes/benzo-fluoranthenes	62				
dibenz(a,j)anthracene	23				
indeno(1,2,3-cd)pyrene	89	12	9	0.3	0.2
dibenz(a,h)anthracene	14				
dibenz(a,c)anthracene	3				
benzo(ghi)perylene	334	85	16	0.8	0.6
anthranthrene	15	11	4	0.1	0.2
methyldibenzanthracenes	203				
dibenzo(b,k)fluoranthene	10				
coronene	60	29	6	0.1	0.1
dibenz(gf,op)naphthacene	41.32				
benzo(rst)pentaphene	7.51				

FUEL RANGES

Source:

Potter, T.L. and K. Simmons (1998). *Total Petroleum Hydrocarbon Criteria Working Group Volume 2: Composition of Petroleum Mixtures.* Amherst Scientific Press, Amherst, MA.

Table C-29
Individual Sample Fuel Mixture Composition Data

Fuel mixture: Crude Oil

Sample #: 14/Prudhoe

From: Riley, R.G., B.L. Thomas, J.W. Anderson, and R.M. Bean, Marine Environmentalist

Compound Class	Carbon #	Compound	Weight Percent	Number of Data Points	Flag (s)
Alkyl-Monoaromatics	7	Toluene	8.2E-02%	1	5
	8	1,2-Diethylbenzene	2.4E-02	1	5
	8	Ethylbenzene	5.6E-02	1	5
	8	m+p-Xylenes	2.0E-01	1	5
	8	o-Xylene	7.9E-02	1	5
	9	1,2,4-Trimethylbenzene	1.1E-01	1	5
	9	1,3,5-Trimethylbenzene	4.1E-02	1	5
	9	Isopropylbenzene	1.6E-02	1	5
	10	1,2,3,5-Tetramethylbenzene	2.7E-02	1	5
	10	1,2,4,5-Tetramethylbenzene	3.8E-02	1	5
	10	1,2-Dimethyl-4-ethylbenzene	2.4E-02	1	5
	10	1,3-Dimethyl-5-ethylbenzene	2.7E-02	1	5
	10	1-Methyl-4-isopropylbenzene	1.2E-02	1	5
	10	Indane	6.7E-02	1	5
	10	sec-Butylbenzene	1.4E-02	1	5
Branched Alkanes	19	Pristane	2.1E-01	1	5
	20	Phytane	1.0E-01	1	5
n-Alkanes	8	n-Octane	4.2E-01	1	5
	9	n-Nonane	4.4E-01	1	5
	10	n-Decane	4.4E-01	1	5
	11	n-Undecane	4.7E-01	1	5
	12	n-Dodecane	4.6E-01	1	5
	13	n-Tridecane	4.5E-01	1	5
	14	n-Tetradecane	4.2E-01	1	5
	15	n-Pentadecane	4.0E-01	1	5
	16	n-Hexadecane	3.7E-01	1	5
	17	n-Heptadecane	3.4E-01	1	5
	18	n-Octadecane	2.5E-01	1	5

Table C-29 (continued)
Individual Sample Fuel Mixture Composition Data

Fuel mixture: Crude Oil

Sample #: 14/Prudhoe

From: Riley, R.G., B.L. Thomas, J.W. Anderson, and R.M. Bean, Marine Environmentalist

Compound Class	Carbon #	Compound	Weight Percent	Number of Data Points	Flag (s)
n-Alkanes	19	n-Nonadecane	3.0E-01	1	5
	20	n-Eicosane	1.9E-01	1	5
	21	n-Heneicosane	1.6E-01	1	5
	22	n-Docosane	1.9E-01	1	5
	23	n-Tricosane	1.7E-01	1	5
	24	n-Tetracosane	1.3E-01	1	5
	25	n-Pentacosane	1.0E-01	1	5
	26	n-Hexacosane	7.6E-02	1	5
Naphthalenes	10	Naphthalene	9.2E-02	1	5
	11	1-Methylnaphthalene	1.3E-01	1	5
	11	2-Methylnaphthalene	1.6E-01	1	5
	12	1,2-Dimethylnaphthalene	4.0E-02	1	5
	12	1,3- & 1,6-Dimethylnaphthalene	8.0E-02	1	5
	12	1,4- & 2,3- & 1,5-Dimethylnaphthalene	8.0E-02	1	5
	12	1,7-Dimethylnaphthalene	1.1E-01	1	5
	12	1- & 2-Ethylnaphthalene	4.8E-02	1	5
	12	2,6- & 2,7-Dimethylnaphthalene	6.9E-02	1	5
	13	2,3,6-Trimethylnaphthalene	5.1E-02	1	5
Polynuclear Aromatics	14	Phenanthrene	3.8E-02	1	5
	15	1-Methylphenanthrene	3.3E-02	1	5
	15	2-Methylphenanthrene	2.1E-02	1	5
	16	3,6-Dimethylphenanthrene	1.1E-02	1	5

Flag(s)

5 Data was converted using formula WT%=mg/kg*10-4.

Table C-30
Individual Sample Fuel Mixture Composition Data

Fuel mixture: Crude Oil

Sample #: 41/Ponca

From: Speight, J.K., 2nd edition, Marcel Dekker, Inc, NYC, NY, 1991

Compound Class	Carbon #	Compound	Weight Percent	Number of Data Points	Flag (s)
Alkyl-Monoaromatics	6	Benzene	2.0E-01	1	1 5
	7	Toluene	5.0E-01	1	1 5
	8	Ethylbenzene	2.0E-01	1	1 5
	8	m+p-Xylenes	8.0E-01	1	1 5
	8	m-Xylene	5.0E-01	1	1 5
	8	o-Xylene	3.0E-01	1	1 5
	8	p-Xylene	1.0E-01	1	1 5
	9	1,2,3-Trimethylbenzene	1.0E-01	1	1 5
	9	1,2,4-Trimethylbenzene	5.1E-01	1	1 5
	9	1,3,5-Trimethylbenzene	1.2E-01	1	1 5
	9	1-Methyl-2-ethylbenzene	9.0E-02	1	1 5
	9	1-Methyl-3-ethylbenzene	1.7E-01	1	1 5
	9	1-Methyl-4-ethylbenzene	6.0E-02	1	1 5
	9	Isopropylbenzene	7.0E-02	1	1 5
	9	n-Propylbenzene	9.0E-02	1	1 5
	10	tert-Butylbenzene	1.0E-02	1	1 5
Branched Alkanes	6	2,2-Dimethylbutane	4.0E-02	1	1 5
	6	2,3-Dimethylbutane	8.0E-02	1	1 5
	6	2-Methylpentane	4.0E-01	1	1 5
	6	3-Methylpentane	3.0E-01	1	1 5
	7	2,3-Dimethylpentane	1.0E-01	1	1 5
	7	3-Ethylpentane	4.0E-03	1	1 5
	7	3-Methylhexane	1.0E-02	1	1 5
	8	2,2,3-Trimethylpentane	6.0E-03	1	1 5
	8	2,2-Dimethylhexane	5.0E-03	1	1 5
	8	2,3,3-Trimethylpentane	6.0E-02	1	1 5
	8	2,3,4-Trimethylpentane	6.0E-02	1	1 5
	8	2,3-Dimethylhexane	6.0E-02	1	1 5

Table C-30 (continued)
Individual Sample Fuel Mixture Composition Data

Fuel mixture: Crude Oil

Sample #: 41/Ponca

From: Speight, J.K., 2nd edition, Marcel Dekker, Inc, NYC, NY, 1991

Compound Class	Carbon #	Compound	Weight Percent	Number of Data Points	Flag (s)
Branched Alkanes	8	2,4 Dimethylhexane	6.0E-02	1	15
	8	2,5 Dimethylhexane	6.0E-02	1	15
	8	2-Methyl-3-heptane	4.0E-02	1	15
	8	3,3-Dimethylhexane	3.0E-02	1	15
	8	Ethylcyclohexane	2.0E-02	1	15
	9	2,3-Dimethylheptane	5.0E-02	1	15
	9	2,6-Dimethylheptane	5.0E-02	1	15
	9	2-Methyloctane	4.0E-02	1	15
	9	3-Methyloctane	1.0E-02	1	15
	9	4-Methyloctane	1.0E-02	1	15
Cycloalkanes	5	Cyclopentane	5.0E-02	1	1 5
	6	Cyclohexane	7.0E-01	1	1 5
Cycloalkanes	6	Methylcyclopentane	9.0E-01	1	1 5
	7	1,1-Dimethylcyclopentane	2.0E-01	1	1 5
	7	cis-1,3-Dimethylcyclopentane	2.0E-01	1	1 5
	7	Ethylcyclopentane	2.0E-01	1	1 5
	7	trans-1,2-Dimethylcyclopentane	5.0E-01	1	1 5
	7	trans-1,3-Dimethylcyclopentane	9.0E-01	1	1 5
	8	1,1,2-Trimethylcyclopentane	6.0E-02	1	1 5
	8	1,1,3-Trimethylcyclopentane	2.0E-01	1	1 5
	8	1,1,3-Trimethylcyclopentane	3.0E-01	1	1 5
	8	trans-1,2-cis-4-Trimethylcyclopentane	3.0E-01	1	1 5
	9	trans-1,2,4-Trimethylcyclohexane	2.0E-01	1	1 5
	9	trans-1,2,4-Trimethylcyclohexane	2.0E-01	1	1 5
n-Alkanes	6	n-Hexane	1.8E+00	1	1 5
	7	n-Heptane	2.3E+00	1	1 5
	8	n-Octane	1.9E+00	1	1 5
	9	n-Nonane	1.8E+00	1	1 5

Table C-30 (continued)
Individual Sample Fuel Mixture Composition Data

Fuel mixture: Crude Oil

Sample #: 41/Ponca

From: Speight, J.K., 2nd edition, Marcel Dekker, Inc, NYC, NY, 1991

Compound Class	Carbon #	Compound	Weight Percent	Number of Data Points	Flag (s)
n-Alkanes	10	n-Decane	1.8E+00	1	1 5
	11	n-Undecane	1.7E+00	1	1 5
	12	n-Dodecane	1.7E+00	1	1 5
Naphthalenes	10	Naphthalene	6.0E-02	1	1 5
	11	1-Methylnaphthalene	1.0E-01	1	1 5
	11	2-Methylnaphthalene	2.0E-01	1	1 5
	11	5-Methyltetralin	8.0E-02	1	1 5
	11	6-Methyltetralin	9.0E-02	1	1 5

Flag(s)

1 Data source was unavailable and data was not reviewed
5 Data was converted using formula WT%=mg/kg*10-4.

Table C-31
Individual Sample Fuel Mixture Composition Data

Fuel mixture: Diesel (#2) Fuel Oil

Sample #: 19/Sample 1910

From: Griest, W. H., E. E. Higgens, and M. R. Guerin, Oak Ridge National Laboratory, Oak Ridge, TN Conf. 851027--5, 1985

Compound Class	Carbon #	Compound	Weight Percent	Number of Data Points	Flag (s)
Alkyl-Monoaromatics	6	Benzene	2.6E-03	1	9
	7	Toluene	2.7E-02	1	9
	8	Ethylbenzene	1.7E-02	1	9
	8	m+p-Xylenes	1.3E-01	1	9
	8	o-Xylene	4.2E-02	1	9
	9	1,3,5-Trimethylbenzene	2.0E-01	1	9
	9	n-Propylbenzene	3.0E-02	1	9
	10	1-Methyl-4-isopropylbenzene	2.6E-02	1	9
	10	n-Butylbenzene	3.1E-02	1	9
	12	3-Methylundecane	1.7E-01	1	9
	13	2-Methyldodecane	2.8E-01	1	9
	14	3-Methyltridecane	2.0E-01	1	9
	15	2-Methyltetradecane	5.5E-01	1	9
	19	Pristane	8.1E-01	1	9
	20	Phytane	5.9E-01	1	9
	13	Fluorene	1.3E-01	1	9
	9	n-Nonane	4.9E-01	1	9
	10	n-Decane	1.0E+00	1	9
	11	n-Undecane	1.7E+00	1	9
	12	n-Dodecane	1.9E+00	1	9
	13	n-Tridecane	2.3E+00	1	9
	14	n-Tetradecane	2.5E+00	1	9
	15	n-Pentadecane	3.1E+00	1	9
	16	n-Hexadecane	2.8E+00	1	9
	17	n-Heptadecane	2.5E+00	1	9
	18	n-Octadecane	2.0E+00	1	9
	19	n-Nonadecane	1.2E+00	1	9
	20	n-Eicosane	5.4E-01	1	9

Table C-31 (continued)
Individual Sample Fuel Mixture Composition Data

Fuel mixture: Diesel (#2) Fuel Oil

Sample #: 19/Sample 1910

From: Griest, W. H., E. E. Higgens, and M. R. Guerin, Oak Ridge National Laboratory, Oak Ridge, TN Conf. 851027--5, 1985

Compound Class	Carbon #	Compound	Weight Percent	Number of Data Points	Flag (s)
Alkyl-Monoaromatics	21	n-Heneicosane	2.3E-01	1	9
Naphthalenes	10	Naphthalene	1.3E-01	1	9
	11	1-Methylnaphthalene	8.1E-01	1	9
	11	2-Methylnaphthalene	1.5E+00	1	9
	12	1,3-Dimethylnaphthalene	1.3E+00	1	9
	12	1,4-Dimethylnaphthalene	2.2E-01	1	9
	12	1,5-Dimethylnaphthalene	3.6E-01	1	9
Polynuclear Aromatics	14	Phenanthrene	2.4E-01	1	9
	15	2-Methylphenanthrene	1.4E-01	1	9
	20	Benzo(a)pyrene	5.0E-06	1	3.4

Flag(s)

3 Data was cited from a secondary source. Original data was not reviewed.
5 Data was converted using formula WT%=ug/g*10-4.
9 Data was converted using formula WT%=mg/g*0.10.

Table C-32
Individual Sample Fuel Mixture Composition Data

Fuel mixture: Diesel (#2) Fuel Oil

Sample #: 19/Sample 1914

From: Griest, W. H., E. E. Higgens, and M. R. Guerin, Oak Ridge National Laboratory, Oak Ridge, TN Conf. 851027--5, 1985

Compound Class	Carbon #	Compound	Weight Percent	Number of Data Points	Flag (s)
Alkyl-Monoaromatics	6	Benzene	8.2E-03	1	9
	7	Toluene	8.3E-02	1	9
	8	Ethylbenzene	4.3E-02	1	9
	8	m+p-Xylenes	2.0E-01	1	9
	8	o-Xylene	7.8E-02	1	9
	9	1,3,5-Trimethylbenzene	9.0E-02	1	9
	9	n-Propylbenzene	4.0E-02	1	9
	10	1-Methyl-4-isopropylbenzene	3.0E-03	1	9
	10	n-Butylbenzene	4.6E-02	1	9
Branched Alkanes	12	3-Methylundecane	9.0E-02	1	9
	13	2-Methyldodecane	2.5E-01	1	9
	14	3-Methyltridecane	2.2E-01	1	9
	15	2-Methyltetradecane	5.8E-01	1	9
	19	Pristane	6.0E-01	1	9
	20	Phytane	5.3E-01	1	9
Diaromatics (Except Naphthalenes)	12	Biphenyl	1.2E-01	1	9
	13	Fluorene	1.2E-01	1	9
n-Alkanes	9	n-Nonane	2.1E-01	1	9
	10	n-Decane	2.8E-01	1	9
	11	n-Undecane	5.7E-01	1	9
	12	n-Dodecane	1.0E+00	1	9
	13	n-Tridecane	2.0E+00	1	9
	14	n-Tetradecane	2.5E+00	1	9
	15	n-Pentadecane	2.5E+00	1	9
	16	n-Hexadecane	2.0E+00	1	9
	17	n-Heptadecane	2.9E+00	1	9
	18	n-Octadecane	1.2E+00	1	9
	19	n-Nonadecane	7.3E-01	1	9

Table C-32 (continued)
Individual Sample Fuel Mixture Composition Data

Fuel mixture: Diesel (#2) Fuel Oil

Sample #: 19/Sample 1914

From: Griest, W. H., E. E. Higgens, and M. R. Guerin, Oak Ridge National Laboratory, Oak Ridge, TN Conf. 851027--5, 1985

Compound Class	Carbon #	Compound	Weight Percent	Number of Data Points	Flag (s)
	20	n-Eicosane	4.0E-01	1	9
	21	n-Heneicosane	2.4E-01	1	9
	10	Naphthalene	2.5E-01	1	9
	11	1-Methylnaphthalene	8.1E-01	1	9
	11	2-Methylnaphthalene	1.4E+00	1	9
	12	1,3-Dimethylnaphthalene	1.2E+00	1	9
	12	1,4-Dimethylnaphthalene	2.3E-01	1	9
	12	1,5-Dimethylnaphthalene	3.6E-01	1	9
	14	Phenanthrene	1.9E-01	1	9
	15	2-Methylphenanthrene	1.7E-01	1	9
	20	Benzo(a)pyrene	1.9E-04	1	3 4

Flag(s)

3 Data was cited from a secondary source. Original data was not reviewed.
4 Data was converted using formula WT%=ug/g*10-4.
9 Data was converted using formula WT%=mg/g*0.10.

Table C-33
Individual Sample Fuel Mixture Composition Data

Fuel mixture: JP-4 Fuel Oil

Sample #: 42/JP-4 Fuel

From: Harper,C.C., O.Faroon and M.A.Melman, Hydrocarbon Contaminated Soils, vol III, E.Calabrese and P.Kostecki, eds., pp 215-241, 1993

Compound Class	Carbon #	Compound	Weight Percent	Number of Data Points	Flag (s)
Alkyl-Monoaromatics	6	Benzene	5.0E-01	1	21
	7	Toluene	1.3E+00	1	21
	8	Ethylbenzene	3.7E-01	1	21
	8	m-Xylene	9.6E-01	1	21
	8	o-Xylene	1.0E+00	1	21
	8	p-Xylene	3.5E-01	1	21
	9	1,2,4-Trimethylbenzene	1.0E+00	1	21
	9	1,3,5-Trimethylbenzene	4.2E-01	1	21
	9	1-Methyl-2-ethylbenzene	2.3E-01	1	21
	9	1-Methyl-3-ethylbenzene	4.9E-01	1	21
	9	1-Methyl-4-ethylbenzene	4.3E-01	1	21
	9	Isopropylbenzene	3.0E-01	1	21
	9	n-Propylbenzene	7.1E-01	1	21
	10	1,2,3,4-Tetramethylbenzene	7.5E-01	1	21
	10	1,2-Dimethyl-4-ethylbenzene	7.7E-01	1	21
	10	1,3-Diethylbenzene	4.6E-01	1	21
	10	1,3-Dimethyl-5-ethylbenzene	6.1E-01	1	21
	10	1,4-Dimethyl-2-ethylbenzene	7.0E-01	1	21
	10	1-Methyl-2-isopropylbenzene	2.9E-01	1	21
	10	1-Methyl-4-propylbenzene	4.0E-01	1	21
Branched Alkanes	4	Isobutane	6.6E-01	1	21
	6	2,2-Dimethylbutane	1.0E-01	1	21
	6	2-Methylpentane	1.3E+00	1	21
	6	3-Methylpentane	8.9E-01	1	21
	7	2,2-Dimethylpentane	2.5E-01	1	21
	7	2-Methylhexane	2.3E+00	1	21
	7	3-Methylhexane	2.0E+00	1	21
	8	2,2,3,3-Tetramethylbutane	2.4E-01	1	21

Table C-33 (continued)
Individual Sample Fuel Mixture Composition Data

Fuel mixture: JP-4 Fuel Oil

Sample #: 42/JP-4 Fuel

From: Harper,C.C., O.Faroon and M.A.Melman, Hydrocarbon Contaminated Soils, vol III, E.Calabrese and P.Kostecki, eds., pp 215-241, 1993

Compound Class	Carbon #	Compound	Weight Percent	Number of Data Points	Flag (s)
Branched Alkanes	8	2,2-Dimethylhexane	7.1E-01	1	21
	8	2,4-Dimethylhexane	5.8E-01	1	21
	8	2,5-Dimethylhexane	3.7E-01	1	21
	8	2-Methylheptane	2.7E+00	1	21
	8	3,3-Dimethylhexane	2.6E-01	1	21
	8	3-Methylheptane	3.0E+00	1	21
	8	4-Methylheptane	9.2E-01	1	21
	9	2,5-Dimethylheptane	5.2E-01	1	21
	9	2-Methyloctane	8.8E-01	1	21
	9	3,4-Dimethylheptane	4.3E-01	1	21
	9	3-Methyloctane	7.9E-01	1	21
	9	4-Ethylheptane	1.8E-01	1	21
	9	4-Methyloctane	8.6E-01	1	21
	12	2-Methylundecane	6.4E-01	1	21
	13	2,6-Dimethylundecane	7.1E-01	1	21
Cycloalkanes	6	Cyclohexane	1.2E+00	1	21
	6	Methylcyclopentane	1.2E+00	1	21
	7	cis-1,2-Dimethylcyclopentane	5.4E-01	1	21
	7	cis-1,3-Dimethylcyclopentane	3.4E-01	1	21
	7	Ethylcyclopentane	2.6E-01	1	21
	7	Methylcyclohexane	2.3E+00	1	21
	7	trans-2,3-Dimethylcyclopentane	3.6E-01	1	21
	8	1,2,3-Trimethylcyclopentane	2.5E-01	1	21
	8	1,2,4-Trimethylcyclopentane	2.5E-01	1	21
	8	cis-1,3-Dimethylcyclohexane	4.2E-01	1	21
	8	Dimethylcyclohexane	4.3E-01	1	21
	9	1,1,3-Trimethylcyclohexane	4.8E-01	1	21
	9	1,3,5-Trimethylcyclohexane	9.9E-01	1	21

Table C-33 (continued)
Individual Sample Fuel Mixture Composition Data

Fuel mixture: JP-4 Fuel Oil

Sample #: 42/JP-4 Fuel

From: Harper,C.C., O.Faroon and M.A.Melman, Hydrocarbon Contaminated Soils, vol III, E.Calabrese and P. Kostecki, eds., pp 215-241, 1993

Compound Class	Carbon #	Compound	Weight Percent	Number of Data Points	Flag (s)
Branched Alkanes	9	1-Methyl-2-ethylcyclohexane	3.9E-01	1	21
	9	1-Methyl-3-ethylcyclohexane	1.7E-01	1	21
	9	1-Methyl-4-ethylcyclohexane	4.8E-01	1	21
n-Alkanes	4	n-Butane	1.2E-01	1	21
	5	n-Pentane	1.1E+00	1	21
	6	n-Hexane	2.2E+00	1	21
	7	n-Heptane	3.7E+00	1	21
	8	n-Octane	3.8E+00	1	21
	9	n-Nonane	2.3E+00	1	21
	10	n-Decane	2.2E+00	1	21
	11	n-Undecane	2.3E+00	1	21
	12	n-Dodecane	2.0E+00	1	21
	13	n-Tridecane	1.5E+00	1	21
	14	n-Tetradecane	7.3E-01	1	21
Naphthalenes	10	Naphthalene	5.0E-01	1	21
	11	1-Methylnaphthalene	7.8E-01	1	21
	11	2-Methylnaphthalene	5.6E-01	1	21
	12	2,6-Dimethylnaphthalene	2.5E-01	1	21

Flags(s) 1 Data source was unavailable and data was not reviewed

Table C-34
Individual Sample Fuel Mixture Composition Data

Fuel mixture: JP-8 Fuel Oil

Sample #: 43/JP-8 Fuel

From: Smith, J.H. et. al., Department of the Air Force, Final Report 54; pp. 1–50; National Technical Information Services, Springfield,VA, A115949/LP, 1981

Compound Class	Carbon #	Compound	Weight Percent	Number of Data Points	Flag (s)
Alkenes	13	Tridecene	7.3E-01	1	21
Alkyl-Monoaromatics	8	m-Xylene	6.0E-02	1	21
	8	o-Xylene	6.0E-02	1	21
	9	1,2,3-Trimethylbenzene	2.7E-01	1	21
	10	1,2,3,4-Tetramethylbenzene	1.1E+00	1	21
	10	1,3-Dimethyl-5-ethylbenzene	6.2E-01	1	21
	10	1-Methyl-2-isopropylbenzene	5.6E-01	1	21
	12	1,2,4-Triethylbenzene	9.9E-01	1	21
	12	1,3,5-Triethylbenzene	6.0E-01	1	21
	13	n-Heptylbenzene	2.5E-01	1	21
	14	n-Octylbenzene	6.1E-01	1	21
	15	1-Ethylpropylbenzene	9.9E-01	1	21
Branched Alkanes	9	3-Methyloctane	4.0E-02	1	21
	10	2,4,6-Trimethylheptane	7.0E-02	1	21
	11	2-Methyldecane	4.1E-01	1	21
	12	2,6-Dimethyldecane	6.6E-01	1	21
	12	2-Methylundecane	1.2E+00	1	21
	13	2,6-Dimethylundecane	2.1E+00	1	21
Cycloalkanes	9	1,1,3-Trimethylcyclohexane	6.0E-02	1	21
	9	1,3,5-Trimethylcyclohexane	6.0E-02	1	21
	9	1-Methyl-4-ethylcyclohexane	1.0E-01	1	21
	9	Propylcyclohexane	1.4E-01	1	21
	10	n-Butylcyclohexane	7.4E-01	1	21
	12	Hexylcyclohexane	9.3E-01	1	21
	12	Phenylcyclohexane	8.7E-01	1	21
	13	Heptylcyclohexane	1.0E+00	1	21
Diaromatics (Except Naphthalenes)	12	Biphenyl	6.3E-01	1	21

Table C-34 (continued)
Individual Sample Fuel Mixture Composition Data

Fuel mixture: JP-8 Fuel Oil

Sample #: 43/JP-8 Fuel

From: Smith, J.H. et. al., Department of the Air Force, Final Report 54; pp. 1–50; National Technical Information Services, Springfield,VA, A115949/LP, 1981

Compound Class	Carbon #	Compound	Weight Percent	Number of Data Points	Flag (s)
n-Alkanes	7	n-Heptane	3.0E-02	1	21
	8	n-Octane	9.0E-02	1	21
	9	n-Nonane	3.1E-01	1	21
	10	n-Decane	1.3E+00	1	21
	11	n-Undecane	4.1E+00	1	21
	12	n-Dodecane	4.7E+00	1	21
	13	n-Tridecane	4.4E+00	1	21
	14	n-Tetradecane	3.0E+00	1	21
	15	n-Pentadecane	1.6E+00	1	21
	16	n-Hexadecane	4.5E-01	1	21
	17	n-Heptadecane	8.0E-02	1	21
	18	n-Octadecane	2.0E-02	1	21

Flag(s)

21 no flag

Table C-35
Individual Sample Fuel Mixture Composition Data

Fuel mixture: Lubricating and Motor Oils

Sample #: 28/Engine Oil/New

From: Grimmer G, J. Jacob, K.-W. Naujack, Fresenius Zeitschrift fur Analytical Chemistry, Vol. 306, pp. 347-355, 1981

Compound Class	Carbon #	Compound	Weight Percent	Number of Data Points	Flag (s)
Other	16	Benzo(b)naptho(2,1-d)thiophene	3.9E-04	1	4
	16	Other Benzonaphthothiophenes	1.4E-04	1	4
	16	Phenanthro(4,4a,4b,5-bcd)thiophene	4.1E-05	1	4
	16	Total Benzonaphthofurans	5.1E-05	1	4
	22	Triphenylene(4,4a,4b,5-bcd)thiophene	1.2E-05	1	4
Polynuclear Aromatics	16	Fluoranthene	7.0E-05	1	4
	16	Pyrene	1.8E-04	1	4
	17	1-Methylpyrene	1.3E-04	1	4
	17	4-Methylpyrene	1.9E-04	1	4
	17	Benzo(a)fluorene	2.7E-04	1	4
	17	Total Benzofluorenes	3.8E-04	1	4
	18	Benz(a)anthracene	3.4E-05	1	4
	18	Chrysene	1.3E-04	1	4
	18	Triphenylene	2.5E-04	1	4
	20	Benzo(a)pyrene	3.0E-06	1	4
	20	Benzo(b)fluoranthene	3.7E-05	1	4
	20	Benzo(e)pyrene	2.5E-05	1	4
	20	Benzo(k)fluoranthene	4.0E-06	1	4
	21	Total Methylbenzo(e)pyrenes	2.6E-05	1	4
	22	Benzo(g,h,i)perylene	7.0E-06	1	4
	22	Dibenz(a,c)anthracene	8.0E-06	1	4
	22	Indeno(1,2,3-cd)pyrene	2.0E-06	1	4

Flag(s)

4 Data was converted using formula WT%=ug/g*10-4.

Table C-36
Individual Sample Fuel Mixture Composition Data

Fuel mixture: Lubricating and Motor Oils

Sample #: 33/Crankcase oil C

From: Peake, E. and K. Parker, Polynuclear Aromatic Hydrocarbons: Chemistry and Biological Effects, pp. 1025–1039, 1980.

Compound Class	Carbon #	Compound	Weight Percent	Number of Data Points	Flag (s)
Alkyl-Monoaromatics		Total Alkyl-Monoaromatics	1.0E-01	1	2 6
Diaromatics (Except Naphthalenes)		Total Fluorenes	3.4E-03	1	2 6
	13	Fluorene	1.7E-04	1	2 6
	13	Total Methylbiphenyls	2.3E-04	1	2 6
	14	Total Methylfluorenes	2.8E-04	1	2 6
	15	Total Dimethylfluorenes	1.4E-04	1	2 6
	16	Total Trimethylfluorenes	1.3E-04	1	2 6
Naphthalenes		Total Naphthalenes	5.0E-02	1	2 6
Other		Total Sulfur Containing Heterocyclics	2.3E-03	1	2 6
	12	Dibenzothiophene	9.0E-05	1	2 6
	13	Total Methyldibenzothiophenes	2.6E-04	1	2 6
	14	Total Dimethyldibenzothiophenes	4.4E-04	1	2 6
	15	Total Trimethyldibenzothiophenes	2.2E-04	1	2 6
	16	Benzonaphthothiophene	3.9E-05	1	2 6
	17	Total Methylbenzonaphthothiophenes	6.2E-05	1	2 6
Polynuclear Aromatics		Terphenyl	1.4E-05	1	2 6
		Total Benzanthracenes/ Chrysenes/Triphenylenes	3.4E-03	1	2 6
		Total Fluoranthenes	6.8E-03	1	2 6
		Total Phenanthrenes	2.5E-02	1	2 6
	14	Anthracene	3.8E-05	1	2 6
	14	Phenanthrene	8.9E-04	1	2 6
	15	Total Methylanthracenes	6.6E-05	1	2 6
	15	Total Methylphenanthrenes	1.3E-03	1	2 6

Table C-36 (continued)
Individual Sample Fuel Mixture Composition Data

Fuel mixture: Lubricating and Motor Oils

Sample #: 33/Crankcase oil C

From: Peake, E. and K. Parker, Polynuclear Aromatic Hydrocarbons: Chemistry and Biological Effects, pp. 1025–1039, 1980.

Compound Class	Carbon #	Compound	Weight Percent	Number of Data Points	Flag (s)
Aromatics	16	Fluoranthene	5.0E-04	1	2 6
	16	Phenylnaphthalene	1.0E-04	1	2 6
	16	Pyrene	7.6E-04	1	2 6
	16	Total Dimethylanthracenes	3.0E-05	1	2 6
	16	Total Dimethylphenanthrenes	1.2E-03	1	2 6
	17	Benzo(a)fluorene	1.1E-04	1	2 6
	17	Benzo(b)fluorene	1.6E-04	1	2 6
	17	Benzo(c)fluorene	5.0E-05	1	2 6
	17	Total Dihydromethylpyrenes	5.1E-05	1	2 6
	17	Total Methylpyrenes	4.8E-04	1	2 6
	17	Total Trimethylanthracenes	5.8E-05	1	2 6
	17	Total Trimethylphenanthrenes	6.9E-04	1	2 6
	18	Benz(a)anthracene	9.9E-05	1	2 6
	18	Benzo(c)phenanthrene	1.4E-05	1	2 6
	18	Total Chrysenes and Triphenylenes	2.8E-04	1	2 6
	18	Total Diethylphenanthrenes	1.4E-04	1	2 6
	18	Total Dimethylpyrenes	1.9E-04	1	2 6
	19	Total Ethylmethylpyrenes	1.6E-05	1	2 6
Polynuclear Aromatics	19	Total Methylbenzo(a)anthracenes	2.8E-0	1	2 6
	20	Benzo(a)pyrene	4.1E-05	1	2 6
	20	Benzo(e)pyrene	2.0E-04	1	2 6
	20	Benzo(k)fluoranthene	1.6E-04	1	2 6
	20	Ethylbenz(a)anthracene	7.4E-05	1	2 6

Table C-36 (continued)
Individual Sample Fuel Mixture Composition Data

Fuel mixture: Lubricating and Motor Oils

Sample #: 33/Crankcase oil C

From: Peake, E. and K. Parker, Polynuclear Aromatic Hydrocarbons: Chemistry and Biological Effects, pp. 1025–1039, 1980.

Compound Class	Carbon #	Compound	Weight Percent	Number of Data Points	Flag (s)
	20	Perylene	1.5E-05	1	2 6
	20	Total Benzpyrenes and Benzfluoranthenes	2.5E-03	1	2 6
	21	Cyclopenta(cd)pyrene	8.9E-05	1	2 6
	21	Methylbenzo(mno)fluoranthene	3.4E-05	1	2 6
	21	Total Ethylcyclopenta(def) phenanthrenes	1.6E-04	1	2 6
	21	Total Methylbenzofluoranthenes	2.1E-05	1	2 6
	21	Total Methylbenzopyrenes	4.7E-05	1	2 6
	22	Benzo(g,h,i)perylene	1.9E-04	1	2 6
	24	Total Benzperylenes	2.7E-03	1	2 6
Total Aromatics		Total Aromatics	2.0E-01	1	2 6

Flag(s)

2 Product has been used in an engine and may have a different composition than a new oil.

6 Data was converted using formula WT%=mg/l*(1/0.8762)*10-4.

Table C-37
Individual Sample Fuel Mixture Composition Data

Fuel mixture: Kerosene Fuel Oil

Sample #: 45/Kjaw&Al-Zaid 1977

From: Goodman, D.R., R.D.Harbison, Division of Interdisciplinary Toxicology, University of Arkansas for Medical Sciences, Little Rock, AK.

Compound Class	Carbon #	Compound	Weight Percent	Number of Data Points	Flag (s)
Alkyl-Monoaromatics	10	1,2,3,4-Tetramethylbenzene	1.1E+00	1	3
Branched Alkanes	10	Isodecane	1.3E+00	1	3
	11	Isoundecane	1.2E+00	1	3
	12	Isododecane	1.2E+00	1	3
	13	Isotridecane	9.0E-01	1	3
	14	Isotetradecane	6.0E-01	1	3
Monoaromatics	10	Tetralin	2.7E-01	1	3
	11	1-Methyltetralin	6.5E-01	1	3
	11	2-Methyltetralin	6.8E-01	1	3
n-Alkanes	8	n-Octane	3.1E+00	1	3
	9	n-Nonane	5.6E+00	1	3
	10	n-Decane	5.6E+00	1	3
	11	n-Undecane	5.6E+00	1	3
	12	n-Dodecane	5.5E+00	1	3
	13	n-Tridecane	2.5E+00	1	3
Naphtalenes	10	Naphthalene	4.6E-01	1	3
	11	1-Methylnaphthalene	8.4E-01	1	3
	11	2-Methylnaphthalene	1.8E+00	1	3

Flag(s)

3 Data was cited from a secondary source. Original data was not reviewed.

Table C-38
Individual Sample Fuel Mixture Composition Data

Fuel mixture: Kerosene Fuel Oil

Sample #: 45/Stucky 1972

From: Goodman, D.R., R.D.Harbison, Division of Interdisciplinary Toxicology, University of Arkansas for Medical Sciences, Little Rock, AK.

Compound Class	Carbon #	Compound	Weight Percent	Number of Data Points	Flag (s)
n-Alkanes	7	n-Heptane	1.4E+00	1	3
	8	n-Octane	1.5E+00	1	3
	9	n-Nonane	4.8E-01	1	3
	10	n-Decane	2.3E+00	1	3
	11	n-Undecane	4.0E+00	1	3
	12	n-Dodecane	2.4E+00	1	3
	13	n-Tridecane	2.1E+00	1	3
	14	n-Tetradecane	2.0E+00	1	3
	15	n-Pentadecane	2.2E+00	1	3

Flag(s)

3 Data was cited from a secondary source. Original data was not reviewed.

Appendix D
LNAPL DATA EVALUATIONS AND CROSS CORRELATIONS

LNAPL DATA EVALUATIONS & CROSS CORRELATIONS

As discussed in the main body of the report, there are many linked relationships between the various principles describing the distribution of LNAPL and other fluids in the pore space and the transport of chemicals away from the LNAPL in the water and vapor phases. This appendix provides some analysis methods to cross-check inputs and assumptions used in calculating LNAPL distribution, mobility, and chemical transport away from the source. This is not intended to be a comprehensive tome, but touches on some key aspects as both an immediate test of assumptions and a starting point for further site specific investigations, as warranted. The appendix is broken up into two broad sections, hydraulics and chemistry, and will focus on use of field information to test key assumptions in the calculation methods. The appendix is presented in no particular priority, as site specific needs will dictate which evaluations may be of use.

SOME PRINCIPLES IN PRACTICE

Following are some bullet points about what the theory and reality suggest you should see in the field under most conditions. If you do not see these things, in general, you would begin to suspect that your site conceptual model requires revision or rethinking.

LNAPL Hydraulics

1. LNAPL plumes will be fully contained and immobilized in a formation volume less than the residual capacity soil volume. Ongoing LNAPL mobility requires an ongoing source or specific geologic conditions such as fractures or zones with high effective LNAPL conductivity.

2. Related to above, LNAPL recovery in the liquid phase is expected to be strongly asymptotic, because as mass is recovered, saturation and effective LNAPL conductivity are decreased. If one does not see this asymptotic decline, it may mean that a large source is in place, or there is a continuing source of product.

3. When LNAPL is observed in monitoring wells, it is present in the formation at concentrations above residual saturation, except possibly under conditions of first lateral entry of LNAPL into water saturated materials. Therefore under most conditions, if geologic sampling suggests relatively small concentrations of LNAPL (e.g., < 5,000 mg/kg for most conditions), you should suspect that sampling did not encounter the intervals in which significant LNAPL resides. Many cases have been observed where changes in groundwater basin management have resulted in “stranding” of LNAPL many tens of feet below current

water table levels. Note that local scale LNAPL mobility does not imply LNAPL plume mobility as a whole.

4. During transient LNAPL pool migration, observed thickness in monitoring wells is expected to show a tailed bell shape through time; thicken quickly during initial release conditions, then diminishing slowly with time and lateral spreading. The timing should also slow significantly with distance away from the release area. Water table variability will skew and overprint these expectations.

5. During transient LNAPL pool migration, a semi-radial gradient mound is expected that may be skewed in the general direction of groundwater flow. It is unusual for free product to closely follow the groundwater gradient in a uniform direction. The magnitude of the LNAPL gradient is expected to slowly diminish through time toward field equilibrium.

6. Multiphase hysteresis, entrapment, and differences between the effective LNAPL conductivity in 2-phase versus 3-phase systems suggest that observed free product thicknesses will be greatest during low water table stands, and vice versa. This condition may or may not manifest itself when the mobility of the free phase is so small that there is effectively permanent disequilibrium in the system. This is expected for fine-grained materials and/or when product saturations in the formation are small.

Dissolved-Phase LNAPL Relationships

1. Dissolved concentrations should decrease upstream to downstream in the source area versus time. Weathering of the fuel is expected to occur most significantly on the upstream side of the source area, and from the top and bottom of the smear zone toward the middle.

2. A dissolved-phase plume in purely high conductivity formations should generally show chromatographic shifts through time with respect to dissolved-phase impacts when the source mass is relatively small. That is, components such as MTBE and benzene should show molar and mass depletion ahead of compounds like xylenes and other, heavier weight molecular compounds.

3. Plumes in interbedded geologic materials may show concentration decreases over time as mass is depleted from permeable zones, but molar shifts in chemistry are likely to be significantly slower because of the slow diffusion of compounds from the fine-grained zones into the coarse-grained horizons. The relative rates depend on the contrast in flow and diffusion characteristics between interbedded materials and the LNAPL saturations in each.

4. Vertical diminishment of LNAPL dissolved-phase concentrations is expected to be significant in the source zone under most conditions, barring a strong downward vertical gradient and flow rate. Thus, if one were to see significant dissolved-phase concentrations at the bottom of monitoring locations in the source zone, one might suspect the vertical extent of LNAPL impacts to be at or below the current screened interval.

LNAPL MOBILITY AND SATURATION RELATIONSHIPS

LNAPL mobility is an important factor in the analysis of LNAPL spills, their risk, and the relative benefits of active mitigation actions. A mobile LNAPL source could impact utilities and other underground structures and cause explosion and flammability dangers. Further, a spread in the LNAPL phase will cause a spread in the groundwater and vapor phase impacts in addition to the chemical transport already in progress in those phases. Mobility is also related to the recoverability of the LNAPL and to the saturation distribution in the pore space. The relationships are linked by interdependent definitions of phase conductivity, transmissivity, saturation, and relative permeability (see the saturation, conductivity, and relative permeability Equations in Appendix A).

Lab Measurements & Data Analysis

There are many laboratory measurements than can be made to assist in evaluations of LNAPL mobility and saturation. Because of the large number of individual methods suited for different materials, saturations, etc., the list given is by category rather than by specific test method. Any qualified petrophysical lab can provide details on specific analyses and their suitability to a particular set of samples. Only primary factors are given below, and other available analyses may assist further interpretation of site geologic conditions affecting LNAPL (e.g., grain-size sorting, bulk density, clay makeup, etc.):

- Capillarity
- Intrinsic permeability
- Native state pore saturation
- Residual phase saturation
- Interfacial tension (water/air, LNAPL/water, LNAPL/air)
- Fluid viscosity
- Phase mobility
- Relative permeability
- Fluid density
- Porosity (effective & total)

One may also use a variety of field data to estimate some of the parameters above. For instance, total petroleum hydrocarbon (TPH) concentrations given in mg/kg can be converted to saturation if one knows, or can estimate, the bulk density of the soil and LNAPL fluid density, as shown below. Note that the equation below assumes the chemical lab has not included soil pore water into their mass concentration results:

$$\theta_o = [TPH]_{mg/kg} \frac{\rho_b(g/cc)}{\rho_o(g/cc)} \cdot 10^{-6} \quad (1) \qquad \overline{S_o} = \frac{\theta_o - \theta_{sr}}{\theta_t - \theta_{sr}} \quad (2)$$

where TPH is the total petroleum hydrocarbon concentration (mg/kg), ρ_o & ρ_b are the LNAPL and soil bulk density, θ_o is the volumetric LNAPL content, θ_t is the total porosity, θ_{sr} is the residual volumetric water content, and $\mathbf{S}_o$ is the oil residual saturation.

One may also estimate a field value of effective LNAPL transmissivity by conducting a hydrocarbon baildown test (Huntley, 1997, 1999), which is similar to an aquifer slug test. Tests are conducted by quickly removing LNAPL from a well, and monitoring the logarithmic rate of recovery. Excerpts of the analysis method are provided below, the original reference provides field examples.

The hydrocarbon baildown test consists of (1) rapid removal of as much of the hydrocarbon in a well as is practical, followed by (2) monitoring of the elevations of the hydrocarbon/air and hydrocarbon/ water interfaces (which will hereafter be referred to as oil/air and oil/water interfaces for expediency) in the monitoring well. This test is applicable only to wells with light, nonaqueous phase liquids (LNAPL) filling a portion of the well casing. In a two-phase system, the flux of hydrocarbon is given by a modified form of Darcy's Law:

$$q_p = k_i k_{r\,n} \frac{\rho_n g}{\mu_n} i \quad (3)$$

where $\mathbf{k}_{rn}$ is the relative permeability of the non-wetting fluid (the hydrocarbon), $\mathbf{k}_i$ is the intrinsic permeability of the soil, ρ_n is the density of the hydrocarbon, $\mathbf{g}$ is the acceleration due to gravity, μ_n is the viscosity of the hydrocarbon, and $\mathbf{i}$ is the gradient.

The relative permeability of the non-wetting phase (k_{rn}) decreases markedly as hydrocarbon saturation decreases, as given by (Mualem, 1976):

$$k_{rn} = \left(1 - S_e\right)^{1/2} \left(1 - S_e^{1/m}\right)^{2m} \quad (4)$$

where $S_e = (S_w - S_{rw})/(S_m - S_{rw})$, $\mathbf{S}_w$ is the water saturation, $\mathbf{S}_{rw}$ is the residual water saturation, $\mathbf{S}_m$ is the

maximum water saturation (equal to 1 for the initial displacement of water by LNAPL and equal to $\mathbf{1-S_{r\,nw}}$ *for displacement of LNAPL by water),* $\mathbf{S_{r\,nw}}$ *is the residual NAPL saturation, and* $\mathbf{m}$ *is a capillary parameter used to fit the measured saturation data to the closed-form van Genuchten expression (van Genuchten, 1980).*

It is clear from this expression that as hydrocarbon saturation decreases (increasing S_w and S_e) the relative permeability of the hydrocarbon phase decreases exponentially. This, together with decreased density and increased viscosity, markedly decreases the mobility of hydrocarbon in the subsurface, both under natural conditions and under conditions of recovery.

As for pure groundwater conditions, the flow of LNAPL into a well is proportional to the effective LNAPL transmissivity. The hydrocarbon baildown test, though not providing any information about "true" or exaggerated thicknesses (as suggested in some literature), does provide very useful information about the mobility of hydrocarbon in the formation. It is apparent that increased hydrocarbon mobility will result in increased rates of recovery following removal of hydrocarbon from a monitoring well. Quantitatively, the rate of recovery of hydrocarbon in the monitoring well will be a function of the hydrocarbon transmissivity (T_o), defined as:

$$T_o = \int_{z_w}^{z_o} k_{ro} k_i \frac{\rho_o g}{\mu_o} dz \quad (5)$$

where $\mathbf{z_o}$ *is the elevation of the oil/air interface and* $\mathbf{z_w}$ *is the elevation of the oil/water interface.*

This hydrocarbon transmissivity can be used to assess recovery rates and lateral rates of mass flux of hydrocarbon.

The hydrocarbon baildown test affects both the hydrocarbon and the ground water in the vicinity of the well. If done carefully, extraction of hydrocarbon from the monitoring well removes little ground water, so ground water pressures in the formation are minimally affected by the test. As hydrocarbon is removed from the well, however, the ground water level in the well rises to correct for the decrease in fluid pressure in the well relative to that of the ground water in the aquifer. Because the mobility of water is typically greater than that of hydrocarbon in the formation near the well, in most cases the potentiometric surface in the well (often called the corrected water table) recovers very rapidly, and thereafter remains constant in the well. This potentiometric surface can be calculated as:

$$z_p = z_w + \rho_r\left(z_o - z_w\right) \qquad (6)$$

where $\mathbf{z_p}$ is the elevation of the potentiometric surface and ρ_r is the relative density of the hydrocarbon.

Therefore, as hydrocarbon enters the well during recovery, the oil/water interface declines to maintain that constant potentiometric surface, then:

$$\Delta z_p = 0 = \Delta z_w + \rho_r\left(\Delta z_o - \Delta z_w\right) \quad (7)$$

or,

$$\Delta z_w = \frac{-\rho_r}{1-\rho_r}\Delta z_o \quad (8)$$

For example, if the hydrocarbon has a relative density of 0.75, then , $\Delta z_w = -3\Delta z_o$, meaning that a 1 meter rise in the oil/air interface elevation will produce a 3 meter drop in the oil/water interface elevation.

Modification of Bouwer-Rice Slug Test Analysis

A hydrocarbon baildown test cannot be analyzed like a simple aquifer slug test, because the volume of hydrocarbon entering the borehole is not simply $\pi r_c^2 \partial h$, it is $\pi r_c^2(\partial z_o - \partial z_w)$, where $\mathbf{r_c}$ is the radius of the casing and $\boldsymbol{h}$ is the change in head. In the case where groundwater mobility is sufficiently high that the potentiometric surface recovers very rapidly, such as that seen in figure 3, equation (6) can be used to relate the change in the oil/water interface elevation to that of the oil/air interface elevation.

Following the approach that Bouwer and Rice used to derive analytic expressions for the analysis of slug tests, the relation between drawdown (s) and discharge (Q) at any point in time can be approximated by the Thiem equation:

$$s = \frac{Q}{2\pi T} ln\left(\frac{r_0}{r_w}\right) \quad (9)$$

where $\mathbf{T}$ is the aquifer transmissivity, $\mathbf{r_o}$ is the radius of influence, and $\mathbf{r_w}$ is the radius of the well.

In a simple water system, $Q = \pi r_c^2 \frac{\partial s}{\partial t}$. In an oil/water system though, we have stated that:

$$Q = \pi r_c^2 \left(\frac{\partial z_o}{\partial t} - \frac{\partial z_w}{\partial t} \right) \quad (10)$$

To solve this, we need a simplifying assumption. If ground water mobility is high relative to water, the potentiometric surface remains relatively constant during the test. Therefore, we can substitute equation (6) into equation (8), resulting in:

$$Q = \pi r_c^2 \left(\frac{1}{1-\rho_r} \right) \left(\frac{\partial z_o}{\partial t} \right) \quad (11)$$

recognizing that $\partial z_0 = -\partial s$, equation (9) can be substituted into equation (7) to produce:

$$s = - \frac{r_c^2 \left(\frac{1}{1-\rho_r} \right) \left(\frac{\partial s}{\partial t} \right)}{2T} ln \left(\frac{r_0}{r_w} \right) \quad (12)$$

rearranging:

$$T \int_0^t \partial t = - \frac{r_c^2 \left(\frac{1}{1-\rho_r} \right)}{2} ln \left(\frac{r_0}{r_w} \right) \int_{s_0}^{s} \left(\frac{\partial s}{s} \right) \quad (13)$$

after integrating from $t = 0$ to $t = t$ and from $s = s_0$ to $s = s$, we have:

$$T = \frac{2.3 r_c^2 \left(\frac{1}{1-\rho_r} \right)}{2t} ln \left(\frac{r_0}{r_w} \right) log \left(\frac{s_0}{s} \right) \quad (14)$$

This, of course, is the same equation as that derived by Bouwer and Rice (1976) for slug test analysis, except for the additional term $(1/(1-\rho_r))$. This implies that a plot of Log (s) versus t will yield a straight line (Figure 4). As in the traditional Bouwer and Rice analysis of slug test data, s_0, the drawdown at $t = 0$, is taken from the graph as the intercept of the straight line fit through the data, and t and s are the coordinates of a second point on the straight line. Transmissivity is calculated using those selected values and equation (12). In other words, the approach is the same as the analysis of Bouwer and Rice, except the transmissivity calculated using the Bouwer and Rice equations is multiplied by $1/(1-\rho_r)$ to arrive at the transmissivity of the hydrocarbon system. This implies that existing aquifer test analysis approaches and software can be used to analyze the data from hydrocarbon baildown tests, with the simple correction of multiplying the resulting transmissivity by $1/(1-\rho_r)$.

It is important to point out that the above approach assumes that the potentiometric surface equilibrate nearly instantly, such that changes in z_w in the monitoring well are related to changes in z_o by eq. (6). If this assumption is not met, substantial error will result.

Approaches Based on Cooper-Jacob Equation

In some cases, either because of limited permeability or a limited length of the well screen below the oil/water interface, the potentiometric surface may not equilibrate rapidly. In this case, the potentiometric surface is rising (recovering) throughout the entire test, such that equation (6) cannot be applied. As a result, the modification of the slug test analysis derived above cannot be used to analyze the LNAPL recovery data. An alternate approach is based on Jacob and Lohman's (1952) modification of the Cooper-Jacob method for constant-drawdown, variable discharge conditions. Jacob and Lohman (1952) noted that, except for very early times, the relationship between decreasing discharge and time, under constant drawdown conditions, is given by:

$$\frac{1}{Q} = \frac{2.3}{4\pi Ts} LOG \frac{2.25Tt}{r^2 S} \qquad (15)$$

*where **Q** is the discharge from the well, **s** is the drawdown (assumed constant), **t** is time, **r** is the distance to the monitoring well (or well radius for a single-well test), and **S** is the aquifer storage coefficient.*

Equation (13) implies that a plot of $1/Q$ versus Log t should be linear, and the slope can be used to calculate the transmissivity by:

$$T = \frac{2.3}{4\pi s\, \Delta(1/Q)} \qquad (16)$$

*where **Δ(1/Q)** is the change in **1/Q** per log cycle.*

Because, during the recovery from a baildown test, the well is not really being pumped, but is recovering from a rapid removal of hydrocarbon from the well, the discharge (Q) must be calculated from the change in volume of hydrocarbon in the well. That is:

$$Q = \frac{\pi r_c^2 \left(\Delta z_o - \Delta z_w\right)}{\Delta t} \qquad (17)$$

The method assumes that drawdown (*s*) is constant during the recovery period and is known. The drawdown for the hydrocarbon baildown test is simply the difference between the original hydrocarbon elevation and the hydrocarbon elevation during the recovery period. For this analysis, we often see three data segments: 1) Early time response of the filter pack material; 2) Early and intermediate time response of the formation under the quasi-constant "drawdown"; 3) Late-time response where the constant drawdown approximation is not met.

Two independent approaches have been derived that allow us to determine hydrocarbon transmissivity from the response of monitoring wells to a hydrocarbon baildown test. In many wells, in our experience, groundwater mobility is sufficiently greater than hydrocarbon mobility that the groundwater potentiometric surface recovers to its original value very rapidly compared to the recovery of the hydrocarbon elevation in the well. In this case, a modification of the Bouwer and Rice (1976) slug test analysis procedure can be applied to the data. However, in those cases where the potentiometric surface does not recover rapidly, this approach will lead to erroneous values of hydrocarbon transmissivity. Under these circumstances, a modification of the Jacob and Lohman (1952) analysis of transient aquifer test data is recommended.

HYDRAULIC SUMMARY

The outlined measurements and tests above are related through various principles (and equations given here and in Appendix A), and can therefore be used as cross-checks on the assumptions of the LNAPL conceptual models used to evaluate a site. Some example problems are provided at the end of this section that isolate simple aspects of various relationships that are important to understanding the LNAPL conceptual model. Significant divergence between values would suggest that the conceptual model is not representative. As with many geologic situations, it is sometimes as important to prove something wrong as it is to prove it right. For instance, as stated earlier, if a site has observable free product and low measured concentrations (e.g., < 5,000 mg/kg), you can bet sampling density was insufficient to characterize the LNAPL plume. This stepwise common sense approach and testing of conceptual assumptions through measurements and observations is critical to generating useful results.

Most of the field versus lab or assumption hydraulic cross-checks rely on interrelationships between saturation, and mobility. For instance, if one assumes a vertically equilibrated system with a corresponding saturation profile, one should see a similar range of measured saturations from the lab.

Based on measured or assumed capillary and permeability properties, one may calculate the LNAPL conductivity and transmissivity, which can in turn be compared to field estimates by baildown testing. If one estimates or calculates an LNAPL profile with an effective transmissivity of less than about 10^{-5} cm^2/sec, one would not expect to see significant accumulations in an observation well. The variety of cause and effect relationships is lengthy, but depend on the simple fundamentals between the primary variables discussed above.

LNAPL CHEMISTRY

As mentioned in the body of the report, for most sites the main indicator of consistency between the LNAPL conceptual model and actual site conditions is the dissolved-phase chemistry through time. That chemistry is directly linked to the LNAPL source and transport conditions, and is essentially a test of the assumptions regarding the distribution, mass and chemistry of the LNAPL in the formation. It is also usually the only time series data available for most sites. So while other indicators may be used, such as vapor phase measurements above the source zone, these are often not available through time with sufficient density. It is also important to recognize that one is looking for statistically relevant trends, and caution should be used when comparing sparse data sets in hydrologically variable settings to the conceptual model. Similarly, trends as opposed to absolute chemistry values are the better indicators of a good conceptual model. For a myriad of reasons, as documented in the report, it would be unusual for a screening model to agree in high detail with site specific concentrations, although general ranges may be consistent. Clearly, the depletion of the source is linked to rates of transport away from that material, and this is the litmus test of importance.

Definition of Mole Fractions of Concern

The most direct method of identifying the mole fractions of various chemicals in the LNAPL source is to collect representative samples for fingerprinting. Most labs can fingerprint using gas chromatography and mass spectrometry. In the absence of free product samples, one may use the dissolved-phase groundwater impacts in the source area to estimate a starting condition for the initial mole fractions of various COCs using Raoult's law (Appendix A). Using benzene as an example, we know the pure phase solubility is about 1,780 mg/l. Since the expected effective concentration is the product of the pure phase solubility and the mole fraction, all that is needed is to divide the site specific effective concentration in the source area by the pure phase solubility to derive the estimated mole fraction. If the effective solubility was 20 mg/l, the corresponding mole fraction would be about 0.01.

For this mole fraction estimate to work, you must use a well or wells in the source area screened in the LNAPL impacted interval. One back check is that the estimated solubility limit for gasoline is typically 60 to 150 mg/l TPH, though this can vary further depending on composition. If site concentrations are smaller than this range, the well may be outside the source zone or the well screen may intersect some "clean" water intervals.

CROSS-RELATIONSHIPS

Now we have in hand several potential cross-relationships that can be used to lend confidence or suspicion to the LNAPL conceptual model built for a particular site. Each is given in bullet format below, as the supporting equations and principles have been provided previously:

1. One may compare the estimated LNAPL transmissivity calculated using lab-derived or assumed parameters to that measured in the field. If the two are in general agreement, perhaps the conceptual model is well suited to the site. If not, one would suspect that the underlying soil and saturation properties assumed for calculations are inaccurate, or that an undefined set of non-ideal conditions is present.

2 One may compare TPH samples in and near the smear zone to the saturation values put into the conceptual model. They should obviously be consistent.

3. One may use inferential measurements, such as laser-fluorescence, to suggest the vertical distribution of hydrocarbons in the subsurface and compare to the vertical discretization in the LNAPL conceptual model. Shape and position are often as useful as hard measurements of saturation or concentration.

4. Vertical profiling of the dissolved-phase groundwater concentrations may suggest whether or not the conceptualization of the vertical distribution of LNAPL is correct. Concentrations should diminish exponentially with depth below the lowest LNAPL/water contact in the formation.

5. Contrasts between the predicted and observed dissolved-phase concentrations in source zone wells are another clear indication of potential conflict between the conceptual model and field conditions, particularly with respect to the shapes of the dissolution curves. Concentration values may be skewed in the field by fine-scale heterogeneity not accounted in calculations, but the general mass depletion trends should be in the ball park. If for instance, the calculations suggest a multi-decade residence time for a particular COC, but periodic groundwater sampling shows statistically relevant decreases of that compound in source zone mass, there is clearly less mass in place than conceptualized.

6. If one recovers liquid-phase hydrocarbons until no further recovery is feasible or demonstrated, one could expect to sample the adjacent formation in the LNAPL interval with the resultant saturation indicative of field residuals.

7. If a cleanup technique is used that targets specific amenable compounds, one should see a molar decrease in those compounds through the time of remediation. A drop in total concentration without a corresponding drop in mole fractions implies that some of the smear zone is not targeted by the particular remediation system.

Appendix E

LNAST SAMPLE INPUT AND OUTPUT FILES

User Input Parameters
(echo of input file structure)

Fine Sand (K= 1 m/day)

1	0.4	0.34	7.5	1.9	0.15	
0.14	3	0.15	0.01	0.003	1	
0.25	0.6944444	0.25				
True		True	True	False	True	False
True		True	True	False	True	
False		True	False	True	False	
0.01	1	10	10	5		

Gasoline

52	24	0.73	0.62			
5						
MTBE	48000	1204	0.11	1	9000	40
Benzene	780	324	0.018	2	90	5
Ethyl Benzene	135	57	0.018	3	65	700
Toluene	515	111	0.079	2.06	60	1000
Xylene	175	38	0.075	2.6	150	10000

Time (yrs)	MTBE	Benzene	Ethyl Benzene	Toluene	Xylene
0.e+0	5.28e+3	3.2e+1	2.43e+0	4.07e+1	1.31e+1
2.74e-7	5.28e+3	3.2e+1	2.43e+0	4.07e+1	1.31e+1
6.02e-7	5.28e+3	3.2e+1	2.43e+0	4.07e+1	1.31e+1
9.97e-7	5.28e+3	3.2e+1	2.43e+0	4.07e+1	1.31e+1
1.47e-6	5.28e+3	3.2e+1	2.43e+0	4.07e+1	1.31e+1
2.04e-6	5.28e+3	3.2e+1	2.43e+0	4.07e+1	1.31e+1
2.72e-6	5.28e+3	3.2e+1	2.43e+0	4.07e+1	1.31e+1
3.54e-6	5.28e+3	3.2e+1	2.43e+0	4.07e+1	1.31e+1
4.52e-6	5.28e+3	3.2e+1	2.43e+0	4.07e+1	1.31e+1

Representative of beginning and ending of a Source Area Dissolved Phase Concentration output file. Files can be several pages long.

3.11e+1	2.8e-45	9.6e-2	1.49e+0	7.95e+0	9.03e+0
3.13e+1	2.8e-45	9.06e-2	1.49e+0	7.81e+0	8.98e+0
3.17e+1	2.8e-45	8.44e-2	1.47e+0	7.64e+0	8.92e+0
3.21e+1	2.8e-45	7.75e-2	1.46e+0	7.45e+0	8.85e+0
3.26e+1	2.8e-45	6.98e-2	1.44e+0	7.23e+0	8.76e+0
3.31e+1	2.8e-45	6.16e-2	1.42e+0	6.96e+0	8.66e+0
3.38e+1	2.8e-45	5.28e-2	1.4e+0	6.66e+0	8.54e+0
3.47e+1	2.8e-45	4.38e-2	1.37e+0	6.3e+0	8.4e+0
3.57e+1	2.8e-45	3.48e-2	1.34e+0	5.9e+0	8.23e+0
3.69e+1	2.8e-45	2.61e-2	1.3e+0	5.45e+0	8.02e+0
3.83e+1	2.8e-45	1.83e-2	1.25e+0	4.95e+0	7.79e+0
4.e+1	2.8e-45	1.18e-2	1.2e+0	4.4e+0	7.51e+0
4.21e+1	2.8e-45	6.66e-3	1.14e+0	3.8e+0	7.18e+0
4.34e+1	2.8e-45	4.93e-3	1.1e+0	3.5e+0	6.99e+0
4.49e+1	2.8e-45	3.38e-3	1.06e+0	3.16e+0	6.77e+0
4.66e+1	2.8e-45	2.11e-3	1.01e+0	2.78e+0	6.51e+0
4.88e+1	2.8e-45	1.15e-3	9.58e-1	2.39e+0	6.21e+0
5.01e+1	2.8e-45	8.35e-4	9.26e-1	2.19e+0	6.04e+0
5.16e+1	2.8e-45	5.61e-4	8.89e-1	1.96e+0	5.83e+0
5.35e+1	2.8e-45	3.39e-4	8.46e-1	1.72e+0	5.6e+0
5.57e+1	2.8e-45	1.78e-4	7.97e-1	1.46e+0	5.32e+0
5.71e+1	2.8e-45	1.27e-4	7.69e-1	1.33e+0	5.16e+0
5.87e+1	2.8e-45	8.33e-5	7.37e-1	1.19e+0	4.98e+0
6.06e+1	2.8e-45	4.88e-5	7.e-1	1.04e+0	4.77e+0
6.29e+1	2.8e-45	2.46e-5	6.57e-1	8.74e-1	4.52e+0

Down-Gradient Extent of Dissolved Phase

Time (yrs)	MTBE	Benzene	Ethyl Benzene	Toluene	Xylene
1.e-2	1.55e+1	8.21e+0			
3.e-2	2.95e+1	1.41e+1			
5.e-2	4.05e+1	2.04e+1			
7.e-2	5.04e+1	2.5e+1		4.08e+0	
9.e-2	5.83e+1	3.01e+1		5.29e+0	
1.1e-1	6.71e+1	3.39e+1		6.16e+0	
1.3e-1	7.64e+1	3.8e+1		6.89e+0	
1.5e-1	8.36e+1	4.18e+1		7.47e+0	
1.7e-1	9.14e+1	4.53e+1		7.89e+0	
1.9e-1	1.e+2	4.9e+1		8.23e+0	
2.1e-1	1.04e+2	5.19e+1		8.49e+0	
2.3e-1	1.09e+2	5.45e+1		8.69e+0	
2.5e-1	1.13e+2	5.72e+1		8.84e+0	
2.7e-1	1.18e+2	6.01e+1		8.96e+0	
2.9e-1	1.24e+2	6.3e+1		9.06e+0	
3.1e-1	1.29e+2	6.61e+1		9.14e+0	
3.3e-1	1.35e+2	6.93e+1		9.2e+0	
3.5e-1	1.41e+2	7.26e+1		9.26e+0	
3.7e-1	1.48e+2	7.56e+1		9.31e+0	

Representative sample of the beginning and end of a Down-Gradient Extent of Dissolved Phase output file.

5.92e+0	1.06e+3	1.21e+2
6.24e+0	1.e+3	1.2e+2
6.56e+0	3.88e+1	1.18e+2
6.88e+0	3.74e+1	1.16e+2
7.2e+0	3.59e+1	1.15e+2
7.52e+0	3.42e+1	1.13e+2
7.84e+0	3.28e+1	1.11e+2
8.32e+0		1.03e+2
8.96e+0		1.e+2
9.6e+0		9.65e+1
1.02e+1		9.28e+1
1.09e+1		8.93e+1
1.15e+1		8.56e+1
1.22e+1		8.2e+1
1.28e+1		7.84e+1
1.34e+1		7.49e+1
1.41e+1		7.31e+1
1.47e+1		7.14e+1
1.54e+1		6.97e+1
1.6e+1		6.79e+1

Fluid Saturation Distribution

z(m)	Sw	So	kw
	1.e+0	0.e+0	1.e+0
.01	1.e+0	4.52e-4	9.21e-1
.02	9.98e-1	1.68e-3	8.55e-1
.03	9.96e-1	3.62e-3	7.95e-1
.04	9.94e-1	6.23e-3	7.39e-1
.05	9.91e-1	9.46e-3	6.87e-1
.06	9.87e-1	1.33e-2	6.38e-1
.07	9.82e-1	1.77e-2	5.93e-1
.08	9.77e-1	2.26e-2	5.5e-1
.09	9.72e-1	2.79e-2	5.1e-1
.1	9.66e-1	3.37e-2	4.72e-1
.11	9.6e-1	4.e-2	4.37e-1
.12	9.53e-1	4.65e-2	4.05e-1
.13	9.47e-1	5.35e-2	3.75e-1
.14	9.39e-1	6.07e-2	3.47e-1
.15	9.32e-1	6.81e-2	3.21e-1
.16	9.24e-1	7.58e-2	2.96e-1
.17	9.16e-1	8.37e-2	2.74e-1
.18	9.08e-1	9.18e-2	2.53e-1
.19	9.e-1	1.e-1	2.34e-1
.2	8.92e-1	1.08e-1	2.17e-1
.21	8.83e-1	1.17e-1	2.e-1
.22	8.75e-1	1.25e-1	1.85e-1
.23	8.66e-1	1.34e-1	1.71e-1

Representative sample of beginning and end of a
Fluid Saturation Distribution output file.
Files can be several pages long depending on input parameters.

1.12	4.38e-1	1.23e-1	0.e+0
1.13	4.36e-1	1.02e-1	0.e+0
1.14	4.34e-1	8.34e-2	0.e+0
1.15	4.32e-1	6.68e-2	0.e+0
1.16	4.3e-1	5.18e-2	0.e+0
1.17	4.28e-1	3.84e-2	0.e+0
1.18	4.26e-1	2.63e-2	0.e+0
1.19	4.25e-1	1.53e-2	0.e+0
1.2	4.23e-1	5.39e-3	0.e+0
1.21	4.21e-1	0.e+0	0.e+0
	0.e+0	0.e+0	0.e+0
	0.e+0	0.e+0	0.e+0
	0.e+0	0.e+0	0.e+0
	0.e+0	0.e+0	0.e+0
	0.e+0	0.e+0	0.e+0

Source Area Dissolved Phase Concentrations

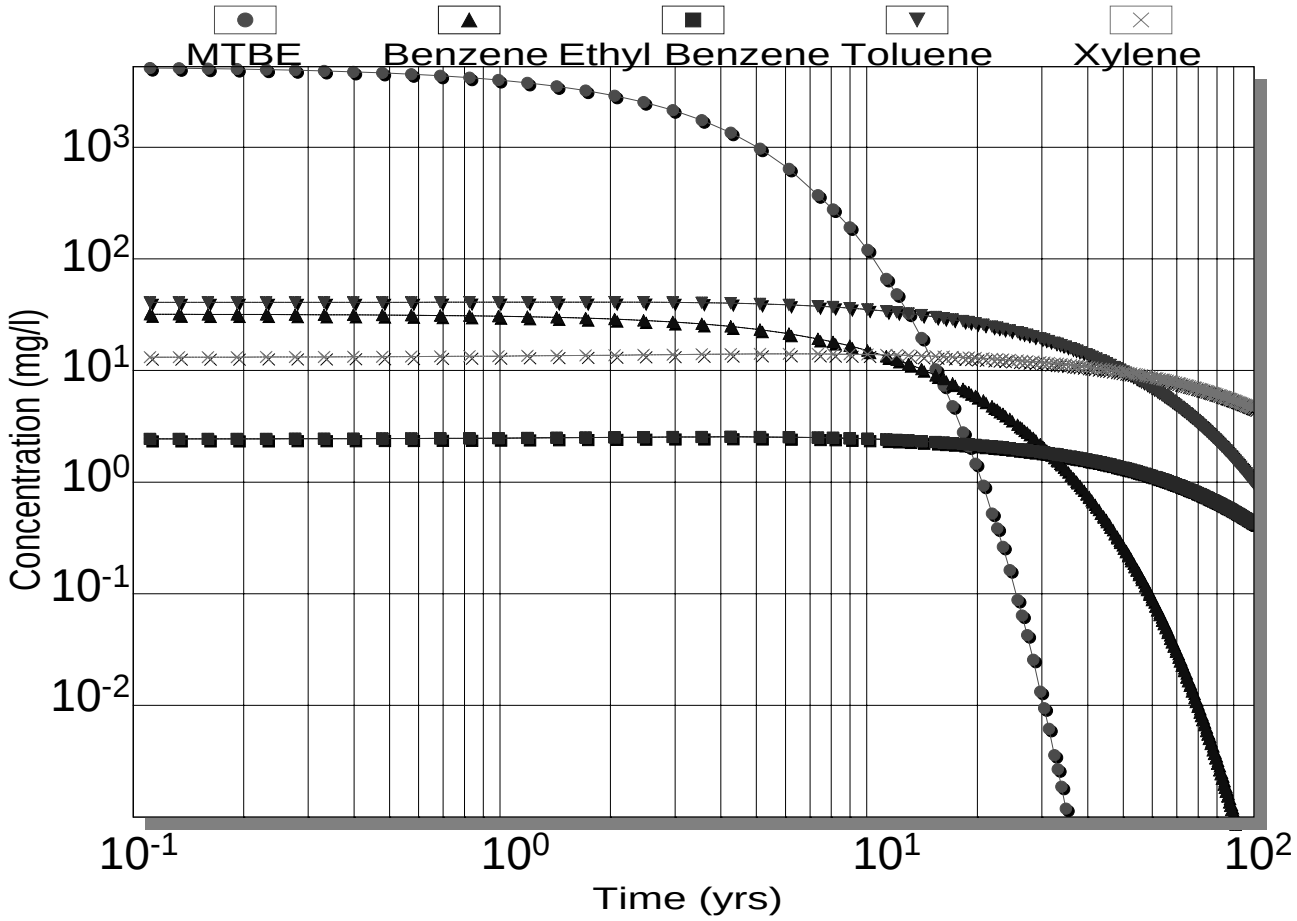

Maximum Downgradient Distance